


RESEARCH ARTICLE

Identification of gene targets of developmental neurotoxicity focusing on DNA hypermethylation involved in irreversible disruption of hippocampal neurogenesis in rats

Satomi Kikuchi^{1,2} | Yasunori Takahashi^{1,2} | Ryota Ojiro^{1,2} | Kazumi Takashima^{1,2} | Hiromu Okano^{1,2} | Qian Tang^{1,2} | Gye-Hyeong Woo³ | Toshinori Yoshida^{1,2} | Makoto Shibutani^{1,2,4} 

¹Laboratory of Veterinary Pathology, Division of Animal Life Science, Institute of Agriculture, Tokyo University of Agriculture and Technology, Tokyo, Japan

²Cooperative Division of Veterinary Sciences, Graduate School of Agriculture, Tokyo University of Agriculture and Technology, Tokyo, Japan

³Laboratory of Histopathology, Department of Clinical Laboratory Science, Semyung University, Jecheon, Republic of Korea

⁴Institute of Global Innovation Research, Tokyo University of Agriculture and Technology, Tokyo, Japan

Correspondence

Makoto Shibutani, Laboratory of Veterinary Pathology, Division of Animal Life Science, Institute of Agriculture, Tokyo University of Agriculture and Technology, 3-5-8 Saiwai-cho, Fuchu-shi, Tokyo 183-8509, Japan.
Email: mshibuta@cc.tuat.ac.jp

Funding information

Japan Society for the Promotion of Science, Grant/Award Number: 18H02341

Abstract

We have previously found that maternal exposure to 6-propyl-2-thiouracil (PTU), valproic acid (VPA), or glycidol (GLY) has a sustained or late effect on hippocampal neurogenesis at the adult stage in rat offspring. Herein, we searched for genes with hypermethylated promoter region and downregulated transcript level to reveal irreversible markers of developmental neurotoxicity. The hippocampal dentate gyrus of male rat offspring exposed maternally to PTU, VPA, or GLY was subjected to Methyl-Seq and RNA-Seq analyses on postnatal day (PND) 21. Among the genes identified, 170 were selected for further validation analysis of gene expression on PND 21 and PND 77 by real-time reverse transcription-PCR. PTU and GLY downregulated many genes on PND 21, reflecting diverse effects on neurogenesis. Furthermore, genes showing sustained downregulation were found after PTU or VPA exposure, reflecting a sustained or late effect on neurogenesis by these compounds. In contrast, such genes were not observed with GLY, probably because of the reversible nature of the effects. Among the genes showing sustained downregulation, *Creb*, *Arc*, and *Hes5* were concurrently downregulated by PTU, suggesting an association with neuronal migration, suppressed synaptic plasticity, and reduction in neural stem and progenitor cells. *Epha7* and *Pvalb* were also concurrently downregulated by PTU, suggesting an association with the reduction in late-stage progenitor cells. VPA induced sustained downregulation of *Vgf* and *Dpysl4*, which may be related to the aberrations in synaptic plasticity. The genes showing sustained downregulation may be irreversible markers of developmental neurotoxicity.

KEYWORDS

6-propyl-2-thiouracil (PTU), developmental neurotoxicity (DNT), gene expression, glycidol (GLY), hippocampal neurogenesis, methylation, rat, valproic acid (VPA)

This is an open access article under the terms of the Creative Commons Attribution-NonCommercial-NoDerivs License, which permits use and distribution in any medium, provided the original work is properly cited, the use is non-commercial and no modifications or adaptations are made.

© 2020 The Authors. Journal of Applied Toxicology published by John Wiley & Sons Ltd.

1 | INTRODUCTION

The hippocampal dentate gyrus of the mammalian brain is crucial for higher brain functions, such as learning and memory, which are closely related to adult hippocampal neurogenesis and activity-dependent synaptic plasticity (Vivar et al., 2013). Adult neurogenesis starts to produce new neurons from the subgranular zone (SGZ) of the dentate gyrus during postnatal life (Zhao et al., 2008). In the hilus of the dentate gyrus, the γ -aminobutyric acid (GABA)ergic interneurons innervate granule cell lineage populations to control SGZ neurogenesis (Masiulis et al., 2011). In addition to inputs by GABAergic interneuron subpopulations, various neuronal populations outside the SGZ create synaptic connections with neurons in the dentate gyrus, such as cholinergic neurons and glutamatergic neurons that are important for maintaining proper proliferation and differentiation of granule cell lineages (Fonnum et al., 1979; Cameron et al., 1995; Zhu et al., 2008).

All the cell populations and their inherent processes involved in the adult neurogenesis may be sensitive targets of developmental neurotoxicity (DNT). Especially, self-renewal of stem cells, proliferation and migration of progenitor cells, neuritogenesis, synaptogenesis, and myelinogenesis may be the developmental processes vulnerable to chemical toxicity. Based on this hypothesis, previously, we have examined the effect of maternal exposure to a number of neurotoxicants on hippocampal neurogenesis and found that all the known neurotoxicants targeted hippocampal neurogenesis under an exposure regimen in accordance with the guidelines for chemicals testing developed by the Organisation for Economic Co-operation and Development (OECD; Test No. 426: Developmental Neurotoxicity Study; OECD, 2007) in rodent animals (Shibutani, 2015). Importantly, some neurotoxicants, such as manganese, aluminum, 6-propyl-2-thiouracil (PTU), glycidol (GLY), and valproic acid (VPA), had a sustained or late effect on neurogenesis in terms of granule cell lineage subpopulations, interneuron subpopulations, and/or other regulatory systems (Wang et al., 2012; Akane, Shiraki et al., 2013; Shiraki et al., 2016; Watanabe et al., 2017; Inohana et al., 2018). If the effect on neurogenesis is permanent in nature, the concern arises regarding learning and memory formation later in life.

Recent studies have indicated that various epigenetic mechanisms, such as alterations in DNA methylation, are involved in the regulation of different aspects of adult neurogenesis (Sun et al., 2011). The idea that DNA methylation is a long-lasting cellular memory necessary for keeping a cellular phenotype has been challenged by discoveries of its dynamic nature (Covic et al., 2010). This relationship is typically seen in CpG sequences at the promoter regions, where DNA methylation can directly interfere with transcription factor binding to DNA or indirectly suppress transcription through methylated DNA-binding proteins that recruit histone deacetylases (HDAC), leading to chromatin condensation and subsequent gene silencing (Jones et al., 1998). Although the effects of epigenetic alterations on neurogenesis have remained unexplored, environmentally induced disruption of DNA methylation warrants

further study (Ceccatelli et al., 2013), given the clear importance of DNA methylation to neuronal development. In fact, exposure to stress (Mueller & Bale, 2008), neurotoxicants (Kundakovic et al., 2013), and maternal neglect (Weaver et al., 2004) in early life have been shown to disrupt epigenetic programming involving DNA methylation in the brain, with lasting consequences for brain gene expression and behavior.

We have recently examined genes showing promoter region hypermethylation in the hippocampal dentate gyrus of mice exposed maternally to manganese, 3,3'-iminodipropionitrile, or hexachlorophene by CpG island (CGI) microarray analysis or methylcapture sequencing analysis (Wang et al., 2013; Watanabe et al., 2018; Tanaka et al., 2019). Among the genes identified, a number of genes showed sustained hypermethylation and transcript downregulation after exposure to these compounds. Interestingly, genes expressed in neural stem cells (NSCs) or neural progenitor cells showed sustained downregulation, whereas those expressed in interneurons mostly showed transient downregulation.

The present study was performed to reveal irreversible DNT markers that can be applied to DNT studies. For this purpose, we focused on hypermethylated genes during the disruption of hippocampal neurogenesis. Because rats are recommended to use in the aforementioned guidelines for testing DNT, we selected PTU, GLY, and VPA as model compounds that have shown irreversible or late effects on hippocampal neurogenesis in rats (Table 1). Hippocampal dentate gyrus was subjected to next generation sequencing analyses in terms of DNA methylation and gene expression at the end of maternal exposure. Selected genes were further examined for transcript expression level changes by real-time reverse transcription-PCR (RT-PCR) analysis to confirm irreversibility of transcript downregulation.

2 | MATERIALS AND METHODS

2.1 | Chemicals and animals

PTU (CAS No. 51-52-5, purity \geq 99%), VPA (sodium salt; CAS No. 1069-66-5, purity \geq 98%), and GLY (CAS No. 556-52-5, purity \geq 96%), were purchased from Sigma-Aldrich Japan Co., Inc. (Tokyo, Japan).

Forty-nine mated female Slc : SD rats were purchased from Japan SLC, Inc. (Hamamatsu, Japan) at gestational day (GD) 1 (appearance of the vaginal plug was designated as GD 0). Rats were individually housed with their offspring in plastic cages with paper bedding until Day 21 post-delivery (where Day 0 is the day of delivery). Animals were maintained in an air-conditioned animal room (temperature: $23 \pm 2^\circ\text{C}$, relative humidity: $55 \pm 15\%$) with a 12-h light/dark cycle, and provided pelleted basal diet (CRF-1; Oriental Yeast Co. Ltd. Tokyo, Japan) throughout the experimental period and tap water until the start of exposure to chemicals ad libitum. From postnatal day (PND) 21 onwards, offspring were reared two or three animals per cage and provided pelleted CRF-1 basal diet and tap water ad libitum.

TABLE 1 Immunohistochemical changes of cellular populations related to hippocampal neurogenesis after maternal exposure to PTU, VPA, or GLY in rats^a

Compound	Target	PND 21	PND 77	References		
PTU	Granule cell lineages	Type-1 NSCs↓		Shiraki et al., 2016		
		Type-2a progenitor cells↓	Type-2a progenitor cells↓			
		Type-3 progenitor cells↓				
		SGZ cell apoptosis↑				
	GABAergic interneurons	RELN ⁺ interneurons↓				
		PVALB ⁺ interneurons↓	PVALB ⁺ interneurons↓ ^b			
		CALB2 ⁺ interneurons↑	CALB2 ⁺ interneurons↑			
		SST ⁺ interneurons↓	SST ⁺ interneurons↑			
	Synaptic plasticity	EPHA4 ⁺ GCL cells↓	EPHA4 ⁺ GCL cells↑			
		ARC ⁺ GCL cells↓	ARC ⁺ GCL cells↑			
VPA	Granule cell lineages		NeuN ⁺ GCL cells↑	Watanabe et al., 2017		
			SGZ cell proliferation↑			
	GABAergic interneurons	RELN ⁺ interneurons↓				
		PVALB ⁺ interneurons↓				
		GAD67 ⁺ interneurons↓	GAD67 ⁺ interneurons↓			
	Synaptic plasticity		ARC ⁺ GCL cells↑			
			COX2 ⁺ GCL cells↑			
	GLY	Granule cell lineages	Immature granule cells↓			Akane, Shiraki et al., 2013 Akane et al., 2014
GABAergic interneurons		NeuN ⁺ interneurons↑	NeuN ⁺ interneurons↑			
		RELN ⁺ immature interneurons↑	RELN ⁺ immature interneurons↑			
		CALB2 ⁺ interneurons↑	CALB2 ⁺ interneurons↑			
Synaptic plasticity			ARC ⁺ GCL cells↑			
			FOS ⁺ GCL cells↑			

Abbreviations: ARC, activity-regulated cytoskeleton-associated protein; CALB2, calbindin-D-29 k (calretinin); COX2, cyclooxygenase 2; EPHA4, EPH receptor A4; FOS, FBJ osteosarcoma oncogene; GABA, γ -aminobutyric acid; GAD67, glutamate decarboxylase 67; GCL, granule cell layer; GLY, glycidol; NeuN, neuronal nuclei; NSC, neural stem cell; PND, postnatal day; PTU, 6-propyl-2-thiouracil; PVALB, parvalbumin; RELN, reelin; SGZ, subgranular zone; SST, somatostatin; VPA, valproic acid.

^aChanges observed at least at the high-dose group are listed in each study.

^bStatistically nonsignificant change as compared with the untreated controls.

2.2 | Experimental design

Mated female rats were randomly divided into four groups of 12–13 animals and were either left untreated (untreated controls; $n = 13$) or treated with PTU at 10 ppm (PTU group; $n = 12$), GLY at 1,000 ppm (GLY group; $n = 12$), or VPA at 2,000 ppm (VPA group; $n = 12$) in drinking water from GD 6 to Day 21 post-delivery. The doses and experimental design were identical to those reported previously (Shiraki et al., 2016; Watanabe et al., 2017; Akane, Shiraki et al., 2013). On PND

4, the litters were randomly culled, leaving eight male offspring per dam. If dams had fewer than eight male pups, more female pups were included to maintain a total of eight pups per litter. Dams and female offspring were euthanized by exsanguination through the abdominal aorta under CO₂/O₂ anesthesia on Day 21 post-delivery. Male offspring were used for gene selection in the hippocampal dentate gyrus, because neurogenesis is influenced by circulating levels of steroid hormones during the estrous cycle (Pawluski et al. 2009). Half of male offspring were subjected to necropsy on PND 21, and the remaining

male offspring were maintained without chemical exposure until PND 77 and subjected to necropsy. Body and brain weights of offspring were measured on the necropsy day. At each time point, 10 or more animals in each group (one or two pups per litter) were selected for future immunohistochemical assessment, and the remaining animals were used for gene selection by means of analyses of DNA methylation and gene expression of transcript levels. During the experimental period, all animals were checked for general conditions regarding nutritional state and signs of abnormal behavior in their home cage in gross observation. Body weight and food and water consumption were measured once or twice per week throughout the study period.

All procedures of the animal experiment were conducted in compliance with the Guidelines for Proper Conduct of Animal Experiments (Science Council of Japan, June 1, 2006) and according to the protocol approved by the Animal Care and Use Committee of Tokyo University of Agriculture and Technology (Approved no.: 30–60). All efforts were made to minimize animal suffering.

2.3 | DNA and RNA extraction

For gene screening and following validation analysis of gene transcript levels on PND 21 and PND 77, 27–32 male offspring per group (2–4 male offspring per dam) were euthanized by exsanguination through the abdominal aorta under CO₂/O₂ anesthesia and subjected to necropsy, and then brains were removed, fixed in methacarn solution for 5 h at 4°C, and then dehydrated in ice-cold absolute ethanol overnight at 4°C, as described previously (Akane, Saito et al., 2013). After dehydration, 2-mm-thick coronal cerebral slices were prepared at the position of –3.5 mm from the bregma. Tissues of the hippocampal dentate gyrus were collected from the slice using a punch biopsy device with a pore-size diameter of 1 mm (Kai Industries Co., Ltd., Gifu, Japan) and stored in ethanol at –80°C until extraction. For analyses of DNA methylation and expression of gene transcript levels, genomic DNA (gDNA) and total RNA were extracted from tissue samples using an Allprep DNA/RNA Mini Kit (Qiagen, Hilden, Germany). Extracted gDNA was used for Methyl-Seq analysis ($n = 5$ from different dams/group, pooled as one sample). Extracted total RNA was used for RNA-Seq analysis ($n = 5$ from different dams/group, pooled as one sample) and real-time RT-PCR analysis ($n = 6$ from different dams/group).

2.4 | Methyl-Seq analysis

To identify PTU, VPA, or GLY-induced DNA methylation changes on PND 21, SureSelect Target Enrichment System (Rat Methyl-Seq; Agilent Technologies, Santa Clara, CA, USA) was implemented according to the manufacturer's protocol (SureSelectXT Methyl-Seq Target Enrichment System, version E0, April 2018). Using the publicly available databases from the University of California Santa Cruz (UCSC) Genome Browser (<http://genome.ucsc.edu>), genomic coordinates for all known CGIs, shores, and shelves in the rat genome were

obtained. Briefly, 0.8 µg of gDNA from each animal was pooled from five animals of each group to prepare one sample. Each pooled gDNA sample was fragmented using a Covaris sonicator (Covaris, Woburn, MA, USA). These fragments were end-repaired, 3'-adenylated, and further ligated with methylated primers. Following hybridization to biotinylated, plus-strand DNA-complementary RNA library 'baits', precipitation from the solution using streptavidin-coated magnetic beads, and RNase-digestion of the baits, captured DNA was bisulfite-converted using the EZ-DNA Methylation-Gold Kit (Zymo Research, Irvine, CA, USA). Subsequently, DNA samples were PCR-amplified using sample-specific indexed ('barcoding') primers to allow for multiplexing and sequenced by 150 bp paired-end sequencing by Illumina NovaSeq 6000 (Illumina, Inc., San Diego, CA, USA) as described in the manufacturer's protocol. After sequencing, the raw sequence reads were filtered based on quality by FastQC v0.11.5 (Babraham Institute, Cambridgeshire, UK). The adapter sequences were also trimmed off the raw sequence reads by Trimmomatic v0.32 (RWTH Aachen University, Aachen, Germany). The trimmed reads were mapped to the reference genome, the *Rattus norvegicus*.rn4.fa (with GA, CT converted Index), which was produced by the Rat Genome Reference Consortium, with BSMAP version 2.87 (<https://code.google.com/archive/p/bsmap/>), which was based on the SOAP (Short Oligo Alignment Program). The only uniquely mapped reads were selected to sort and index, and PCR duplicates were removed with SAMBAMBA version 0.5.9 (<http://lomereiter.github.io/sambamba/>). The methylation ratio of every single cytosine location within the on-target region was extracted from the mapping results using 'methylation.py' script in BSMAP. The results of the coverage profiles were calculated as number of C/effective CT counts for each cytosine in CpG.

Genes showing CpG site hypermethylation up to 2-kb upstream from the transcription start site were selected with the criterion of the methylation ratio of ≥ 0.2 in each treatment group sample as compared with the untreated control sample.

2.5 | RNA-Seq analysis

Whole transcriptome sequencing was performed to identify PTU, VPA, or GLY-induced transcript-level expression changes on PND 21. TruSeq Stranded mRNA LT Sample Prep Kit (Illumina, Inc.) was used to sample preparation according to the manufacturer's protocol (TruSeq Stranded mRNA Sample Preparation Guide Part #1531047 Rev. E, October 2013). Using the publicly available databases from the UCSC Genome Browser (<http://genome.ucsc.edu>), genomic coordinates in the rat genome were obtained. Briefly, 0.4 µg of total RNA from each animal was pooled from five animals of each group to prepare one sample. DNA contamination was eliminated using DNase. The poly-A containing mRNA molecules were purified using poly-T oligo-attached magnetic beads. The fragments of purified RNA were reverse-transcribed into complementary DNA (cDNA). Adapters were ligated onto both ends of the cDNA fragments. After amplifying fragments using PCR,

fragments with insert sizes between 200 and 400 bp were selected. Subsequently, cDNA fragments were PCR-amplified using sample-specific indexed (barcoding) primers to allow for multiplexing and sequenced by 100 bp paired-end sequencing by Illumina NovaSeq 6000 as described in the manufacturer's protocol. After sequencing, the raw sequence reads were filtered based on quality by FastQC version 0.11.7 (Babraham Institute). The adapter sequences were also trimmed off the raw sequence reads by Trimmomatic version 0.32 (RWTH Aachen University). The trimmed reads were assembled by StringTie version 1.3.3b (Johns Hopkins University, Baltimore, MD, USA) and mapped to the reference genome, the *Rattus norvegicus*.rn6.fa (with GA, CT converted Index), which was produced by the Rat Genome Reference Consortium with HISAT2 version 2.0.5, Bowtie 2 version 2.3.4.1 (Johns Hopkins University) splice-aware aligner. Expression profiles were represented as read count and normalized value as fragments per kilobase of transcript per million mapped (FPKM) reads, which was based on transcript length and depth of coverage. The difference per comparison pair was expressed as 'fc.', the fold change between the $\log_2(1 + \text{FPKM})$ value of the each chemical exposure group and that of the untreated controls.

Genes showing downregulation were selected with the criterion of the fc. of ≤ -1 as compared with the untreated controls, and gene ontology-based functional annotation analysis was performed using the Database for Annotation, Visualization and Integrated Discovery (DAVID), version 6.7 (Huang et al., 2009a, b) to clarify biological functions.

2.6 | Real-time RT-PCR analysis

Real-time RT-PCR quantification of transcript level was performed for genes selected as being hypermethylated in Methyl-Seq analysis, downregulated in RNA-Seq analysis, and related to the nervous system in functional annotation analysis. Around 50 to 60 genes that have been investigated the functional role in nervous system development and differentiation were selected per compound from those showing profound downregulation of transcript level in RNA-Seq analysis. For genes whose downregulation of transcript levels was confirmed on PND 21, expression on PND 77 was also analyzed. First-strand complementary DNA was synthesized using SuperScript[®] III Reverse Transcriptase (Thermo Fisher Scientific, Waltham, MA, USA) in a 20- μ l total reaction mixture with 0.6 μ g of total RNA. Analysis of the transcript levels for the candidate genes shown in Table S1 was performed using PCR primers designed with Primer Express software version 3.0 (Thermo Fisher Scientific). Real-time PCR with Power SYBR[®] Green PCR Master Mix (Thermo Fisher Scientific) was conducted using a StepOnePlus[™] Real-time PCR System (Thermo Fisher Scientific). The relative differences in gene expression between the untreated controls and each treatment group were calculated using threshold cycle (C_T) values that were first normalized to that of *Gapdh* or *Hprt1*, which served as endogenous controls in the same sample, and then relative to a C_T value of

the untreated controls using the $2^{-\Delta\Delta C_T}$ method (Livak and Schmittgen, 2001).

2.7 | Statistical analysis

Numerical data were presented as the mean \pm SD. Body weights, brain weights, and transcript expression data of offspring were analyzed using the litter as the experimental unit. Other data were analyzed using the individual animal as the experimental unit. Data were analyzed using Levene's test for homogeneity of variance. If the variance was homogenous in the analysis of data from four groups, that is, body and brain weights, food and water consumption, and reproductive parameters, numerical data were evaluated using Dunnett's test for comparisons between the untreated controls and each treatment group. For heterogeneous data, Aspin-Welch's *t* test with Bonferroni correction was used. If the variance was homogenous in the analysis of data from two groups, that is, transcript-level expression, numerical data were evaluated using Student's *t* test. When data were heterogeneous, Aspin-Welch's *t* test was used. All analyses were performed using the IBM SPSS Statistics version 25 (IBM Corporation, Armonk, NY, USA), and $p < 0.05$ was considered statistically significant.

3 | RESULTS

3.1 | Maternal parameters

In the present study, there were two and one nonpregnant females in the untreated controls and GLY group, respectively.

In the PTU group, there were no abnormal clinical signs during the experimental period. Body weight was significantly decreased on PND 12 compared with the untreated controls (Figure S1A). Food consumption was significantly decreased on GD 20 and from PND 5 to PND 20 compared with the untreated controls (Figure S1B). Water consumption was significantly decreased from GD 20 to PND 20 compared with the untreated controls (Figure S1C). Maternal exposure to PTU did not affect reproductive parameters (Table S2).

In the VPA group, there were no abnormal clinical signs during the experimental period. Body weight was significantly decreased on PND 12 compared with the untreated controls (Figure S1A). Food consumption was significantly decreased on PND 9 and PND 16 compared with the untreated controls (Figure S1B). Water consumption was significantly decreased from GD 14 to GD 20 and from PND 5 to PND 20 compared with the untreated controls (Figure S1C). Maternal exposure to VPA did not affect reproductive parameters (Table S2).

Dams exposed to GLY exhibited abnormal gait after PND 12. Body weight was significantly decreased from GD 20 to PND 21 compared with the untreated controls (Figure S1A). Food consumption was significantly decreased from GD 20 to PND 20 compared with the untreated controls (Figure S1B). Water consumption was significantly decreased from GD 7 to PND 20 compared with the untreated

controls (Figure S1C). Maternal exposure to GLY did not affect reproductive parameters (Table S2).

3.2 | Clinical observations and necropsy data of offspring

In the PTU group, there were no abnormal clinical signs during the experimental period. Body weight was significantly decreased from PND 4 to PND 77 compared with the untreated controls (Figure S2A). Food and water consumption were significantly decreased from PND 28 to PND 56 compared with the untreated controls (Figure S2B,C). Body and brain weights were decreased at necropsies on PND 21 and PND 77 compared with the untreated controls (Table S3).

In the VPA group, there were no abnormal clinical signs during the experimental period. Body weight was significantly decreased on PND 4 and PND 8 and from PND 15 to PND 28 compared with the untreated controls (Figure S2A). There were no significant changes in food and water consumption between the VPA group and the untreated controls (Figure S2B,C). Body weight was decreased at necropsy on PND 21 compared with the untreated controls (Table S3).

In the GLY group, there were no abnormal clinical signs during the experimental period. Body weight was significantly decreased from PND 4 to PND 77 compared with the untreated controls (Figure S2A). Food and water consumption were significantly decreased from PND 28 to PND 42 compared with the untreated controls (Figure S2B,C). Body and brain weights were decreased at necropsies on PND 21 and PND 77 compared with the untreated controls (Table S3).

3.3 | Hypermethylated and downregulated genes in the hippocampal dentate gyrus

The metrics for the high-throughput sequencing of samples were shown in Tables S4 and S5. The numbers of genes showing hypermethylation and downregulation by Methyl-Seq and RNA-Seq analyses were shown in Figure 1. Total of 1,220, 429, and 805 genes showed promotor-region hypermethylation (difference in the methylation ratio ≥ 0.2 as compared with the untreated controls) and downregulation of the transcript level (difference in the $fc. \leq -1$ as compared with the untreated controls) on PND 21 by maternal exposure to PTU, VPA, and GLY, respectively. There were 77 genes in common with all 3 compounds, 84 genes in common with both PTU and VPA, 313 genes in common with both PTU and GLY, and 40 genes in common with both VPA and GLY (Figure 1A). Among the hypermethylated and downregulated genes, 249, 81, and 183 genes were related to the nervous system in the PTU, VPA, and GLY by functional annotation investigation using DAVID version 6.7, respectively. There were 18 genes in common with all 3 compounds, 9 genes in common with both PTU and VPA, 65 genes in common with both PTU and GLY, and 7 genes in common with both VPA and GLY (Figure 1B).

3.4 | Transcript expression changes of candidate genes

Among the hypermethylated and downregulated genes, 61, 50, and 59 genes were selected for validation analysis of transcript levels by real-time RT-PCR in comparison with the untreated controls in the

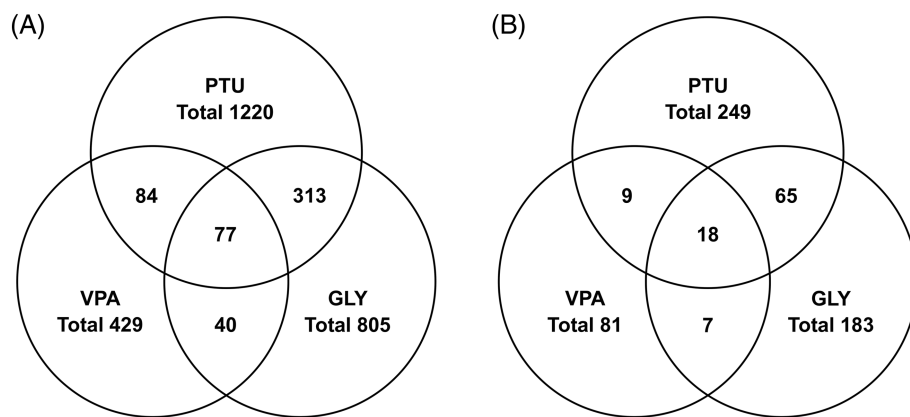


FIGURE 1 Venn diagram denoting the number of genes showing promotor-region hypermethylation and transcript downregulation by means of Methyl-Seq and RNA-Seq analyses on PND 21. (A) Total number of genes obtained. (B) Number of nervous system-related genes selected by functional annotation

TABLE 2 Number of genes validated for downregulation of transcript level by real-time reverse transcription-PCR (RT-PCR)

Variable	PTU	VPA	GLY	Common to all three chemicals	Common to PTU and VPA	Common to PTU and GLY	Common to VPA and GLY
Selected for validation analysis	61	50	59	13	6	21	6
Downregulated at PND 21	39	7	23	0	1	10	1
Downregulated at PND 77	12	3	0	0	0	0	0

Abbreviations: GLY, glycidol; PTU, 6-propyl-2-thiouracil; RT, reverse transcription; VPA, valproic acid.

TABLE 3 List of validated genes for transcript-level downregulation on PND 21 and transcript levels of expression on PND 21 and PND 77 after developmental exposure to PTU

Gene	PND 21				PND 77			
	Control		PTU		Control		PTU	
	Normalized by		Normalized by		Normalized by		Normalized by	
	Gapdh	Hprt1	Gapdh	Hprt1	Gapdh	Hprt1	Gapdh	Hprt1
Arc	1.03 ± 0.27	1.03 ± 0.29	0.33 ± 0.22**	0.33 ± 0.20**	1.00 ± 0.10	1.00 ± 0.08	0.53 ± 0.20**	0.52 ± 0.12**
Bmp3	1.10 ± 0.51	1.04 ± 0.30	0.50 ± 0.26*	0.39 ± 0.20**	1.03 ± 0.29	1.01 ± 0.17	0.59 ± 0.22*	0.83 ± 0.39
Cebpb	1.02 ± 0.23	1.03 ± 0.28	0.58 ± 0.14**	0.55 ± 0.14**	1.02 ± 0.19	1.01 ± 0.16	0.77 ± 0.15*	0.79 ± 0.16*
Creb1	1.02 ± 0.21	1.01 ± 0.16	0.83 ± 0.14	0.79 ± 0.13*	1.01 ± 0.15	1.00 ± 0.05	0.79 ± 0.09*	1.08 ± 0.12
Epha7	1.02 ± 0.23	1.02 ± 0.24	0.46 ± 0.13**	0.43 ± 0.09**	1.02 ± 0.20	1.01 ± 0.19	0.72 ± 0.16*	0.73 ± 0.16*
Fgf13	1.04 ± 0.33	1.01 ± 0.17	0.69 ± 0.26	0.54 ± 0.20**	1.00 ± 0.08	1.00 ± 0.10	0.64 ± 0.03**	0.87 ± 0.08*
Fzd9	1.01 ± 0.17	1.01 ± 0.16	0.67 ± 0.17**	1.06 ± 0.20	1.01 ± 0.16	1.00 ± 0.09	0.75 ± 0.28	0.74 ± 0.11**
Hes5	1.02 ± 0.26	1.02 ± 0.25	0.62 ± 0.10*	1.01 ± 0.15	1.00 ± 0.07	1.01 ± 0.12	0.82 ± 0.20	0.83 ± 0.13*
Mas1	1.02 ± 0.23	1.02 ± 0.23	0.68 ± 0.42	0.52 ± 0.31*	1.01 ± 0.18	1.01 ± 0.13	0.77 ± 0.09*	1.05 ± 0.12
Pvalb	1.05 ± 0.40	1.06 ± 0.47	0.26 ± 0.08**	0.25 ± 0.06**	1.01 ± 0.12	1.00 ± 0.06	0.59 ± 0.14**	0.59 ± 0.06**
Reln	1.04 ± 0.31	1.03 ± 0.31	0.77 ± 0.11	0.72 ± 0.11*	1.02 ± 0.19	1.01 ± 0.12	0.73 ± 0.09**	0.99 ± 0.17
Sema3c	1.02 ± 0.19	1.01 ± 0.16	0.09 ± 0.03**	0.15 ± 0.05**	1.01 ± 0.17	1.01 ± 0.15	0.47 ± 0.18**	0.46 ± 0.07**
Acsl4	1.01 ± 0.15	1.01 ± 0.15	0.78 ± 0.10*	0.74 ± 0.08**	1.01 ± 0.16	1.01 ± 0.13	0.97 ± 0.17	0.99 ± 0.08
Arhgef2	1.03 ± 0.30	1.00 ± 0.10	0.73 ± 0.16	0.59 ± 0.22**	1.00 ± 0.07	1.00 ± 0.04	1.12 ± 0.20	1.15 ± 0.15
Atp2b2	1.01 ± 0.19	1.02 ± 0.23	0.58 ± 0.05**	0.55 ± 0.07**	1.01 ± 0.11	1.00 ± 0.05	1.16 ± 0.21	1.18 ± 0.21
Baiap2	1.03 ± 0.27	1.02 ± 0.22	0.69 ± 0.20*	0.65 ± 0.18**	1.01 ± 0.15	1.01 ± 0.12	0.88 ± 0.12	0.90 ± 0.12
Cntn2	1.03 ± 0.30	1.03 ± 0.29	0.45 ± 0.09**	0.42 ± 0.08**	1.01 ± 0.15	1.00 ± 0.08	1.54 ± 0.40*	1.55 ± 0.09**
Dab2ip	1.02 ± 0.23	1.02 ± 0.22	0.78 ± 0.17	0.72 ± 0.09*	1.01 ± 0.16	1.00 ± 0.09	0.99 ± 0.07	1.36 ± 0.15
Dao	1.06 ± 0.42	1.04 ± 0.32	0.45 ± 0.31*	0.43 ± 0.23**	1.19 ± 0.61	1.17 ± 0.59	1.74 ± 1.18	2.38 ± 1.61
Dll4	1.02 ± 0.21	1.01 ± 0.18	0.74 ± 0.14*	0.69 ± 0.15**	1.03 ± 0.26	1.02 ± 0.25	0.96 ± 0.19	1.01 ± 0.31
Epha5	1.03 ± 0.27	1.04 ± 0.30	0.45 ± 0.23**	0.42 ± 0.19**	1.00 ± 0.08	1.01 ± 0.13	0.99 ± 0.23	1.00 ± 0.14
Fgf2	1.08 ± 0.48	1.07 ± 0.42	0.49 ± 0.08*	0.46 ± 0.05*	1.02 ± 0.20	1.02 ± 0.20	0.99 ± 0.24	1.00 ± 0.15
Id2	1.01 ± 0.17	1.01 ± 0.14	0.73 ± 0.21*	0.66 ± 0.11**	1.01 ± 0.19	1.01 ± 0.14	0.86 ± 0.22	0.86 ± 0.12
Igf1	1.01 ± 0.16	1.01 ± 0.14	0.77 ± 0.08**	1.24 ± 0.18*	1.02 ± 0.21	1.01 ± 0.19	1.65 ± 0.31**	1.72 ± 0.44**
Ndel1	1.01 ± 0.14	1.01 ± 0.16	0.81 ± 0.13*	0.75 ± 0.04*	1.00 ± 0.05	1.00 ± 0.03	0.90 ± 0.14	0.92 ± 0.11
Neurod6	1.01 ± 0.17	1.02 ± 0.23	0.48 ± 0.40*	0.44 ± 0.34**	1.01 ± 0.13	1.01 ± 0.18	0.85 ± 0.25	0.85 ± 0.08
Numbl	1.04 ± 0.30	1.03 ± 0.25	0.89 ± 0.17	0.70 ± 0.16*	1.00 ± 0.06	1.00 ± 0.06	1.03 ± 0.14	1.06 ± 0.13
Ptpru	1.11 ± 0.57	1.11 ± 0.57	0.45 ± 0.10*	0.73 ± 0.17	1.01 ± 0.18	1.01 ± 0.17	0.86 ± 0.20	0.88 ± 0.14
Robo3	1.02 ± 0.22	1.02 ± 0.24	0.06 ± 0.02**	0.06 ± 0.03**	1.01 ± 0.18	1.01 ± 0.17	0.91 ± 0.1	0.94 ± 0.17
Ror2	1.06 ± 0.40	1.04 ± 0.34	0.63 ± 0.14*	0.58 ± 0.07*	1.02 ± 0.23	1.02 ± 0.23	1.06 ± 0.24	1.08 ± 0.20
Shh	1.07 ± 0.42	1.06 ± 0.38	0.53 ± 0.16*	0.51 ± 0.21*	1.03 ± 0.28	1.03 ± 0.30	1.50 ± 0.51	1.57 ± 0.60
Six4	1.10 ± 0.51	1.15 ± 0.66	0.53 ± 0.16*	0.51 ± 0.14*	1.02 ± 0.24	1.02 ± 0.22	1.43 ± 0.40	1.46 ± 0.36*
Tfap2c	1.05 ± 0.34	1.04 ± 0.32	0.37 ± 0.16**	0.60 ± 0.27*	1.09 ± 0.52	1.08 ± 0.49	0.95 ± 0.27	1.27 ± 0.31
Thrsp	1.05 ± 0.34	1.01 ± 0.16	0.47 ± 0.09**	0.37 ± 0.09**	1.01 ± 0.18	1.01 ± 0.14	1.01 ± 0.24	1.02 ± 0.11
Vegfa	1.10 ± 0.58	1.03 ± 0.31	0.84 ± 0.14	0.68 ± 0.19*	1.02 ± 0.21	1.01 ± 0.17	1.25 ± 0.25	1.27 ± 0.12*
Wnt7b	1.10 ± 0.54	1.03 ± 0.28	0.66 ± 0.10	0.53 ± 0.14**	1.02 ± 0.21	1.01 ± 0.15	1.25 ± 0.23	1.28 ± 0.17*
Wnt8b	1.07 ± 0.43	1.06 ± 0.43	0.62 ± 0.17	0.50 ± 0.22*	1.02 ± 0.22	1.03 ± 0.27	1.01 ± 0.57	0.97 ± 0.32
Wnt9a	1.13 ± 0.66	1.06 ± 0.40	0.56 ± 0.11	0.45 ± 0.12**	1.07 ± 0.43	1.07 ± 0.41	0.79 ± 0.10	0.81 ± 0.14
Wnt16	1.06 ± 0.36	1.05 ± 0.31	0.51 ± 0.20**	0.41 ± 0.23**	1.03 ± 0.26	1.02 ± 0.23	1.04 ± 0.24	1.09 ± 0.35

Note. Data are expressed as the mean \pm SD ($n = 6$ /group).

Abbreviations: *Acsl4*, acyl-CoA synthetase long-chain family member 4; *Arc*, activity-regulated cytoskeleton-associated protein; *Arhgef2*, Rho guanine nucleotide exchange factor 2; *Atp2b2*, ATPase plasma membrane Ca^{2+} transporting 2; *Baiap2*, BAR/IMD domain containing adaptor protein 2; *Bmp3*, bone morphogenetic protein 3; *Cebpb*, CCAAT/enhancer-binding protein beta; *Cntn2*, contactin 2; *Creb1*, cAMP-responsive element-binding protein 1; *Dab2ip*, DAB2-interacting protein; *Dao*, D-amino-acid oxidase; *Dll4*, delta-like canonical Notch ligand 4; *Epha5*, EPH receptor A5; *Epha7*, Eph receptor A7; *Fgf2*, fibroblast growth factor 2; *Fgf13*, fibroblast growth factor 13; *Fzd9*, frizzled class receptor 9; *Gapdh*, glyceraldehyde-3-phosphate dehydrogenase; *Hes5*, hes family bHLH transcription factor 5; *Hprt1*, hypoxanthine phosphoribosyltransferase 1; *Id2*, inhibitor of DNA-binding 2; *Igf1*, insulin-like growth factor 1; *Mas1*, MAS1 proto-oncogene, G protein-coupled receptor; *Ndel1*, nudE neurodevelopment protein 1-like 1; *Neurod6*, neuronal differentiation 6; *Numbl*, NUMB-like, endocytic adaptor protein; PND, postnatal day; *Ptpru*, protein tyrosine phosphatase, receptor type, U; PTU, 6-propyl-2-thiouracil; *Pvalb*, parvalbumin; *Reln*, reelin; *Robo3*, roundabout guidance receptor 3; *Ror2*, receptor tyrosine kinase-like orphan receptor 2; *Sema3c*, semaphorin 3C; *Shh*, sonic hedgehog signaling molecule; *Six4*, SIX homeobox 4; *Tfap2c*, transcription factor AP-2 gamma; *Thrsp*, thyroid hormone responsive; *Vegfa*, vascular endothelial growth factor A; *Wnt7b*, Wnt family member 7B; *Wnt8b*, Wnt family member 8B; *Wnt9a*, Wnt family member 9A; *Wnt16*, Wnt family member 16.

* $p < 0.05$ ** $p < 0.01$, significantly different from the untreated controls by Student's or Aspin-Welch's t test.

PTU, VPA, and GLY, respectively (Table 2 and S6–S11). Among them, transcript downregulation was confirmed with 39, 7, and 23 genes on PND 21 in the PTU, VPA, and GLY, respectively (Tables 2–5). On PND 77, the downregulation was further sustained with 12, 3, and 0 genes in the PTU, VPA, and GLY, respectively. In the PTU group, transcript levels of *Arc*, *Bmp3*, *Cebpb*, *Creb1*, *Epha7*, *Fgf13*, *Fzd9*, *Hes5*, *Mas1*, *Pvalb*, *Reln*, and *Sema3c* were significantly decreased compared with the untreated controls on both PND 21 and PND 77 (Table 3). In this group, transcript levels of *Acsl4*, *Arhgef2*, *Atp2b2*, *Baiap2*, *Cntn2*, *Dab2ip*, *Dao*, *Dll4*, *Epha5*, *Fgf2*, *Id2*, *Igf1*, *Ndel1*, *Neurod6*, *Numbl*, *Ptpru*, *Robo3*, *Ror2*, *Shh*, *Six4*, *Tfap2c*, *Thrsp*, *Vegfa*, *Wnt7b*, *Wnt8b*, *Wnt9a*, and *Wnt16* were significantly decreased only on PND 21 compared with the untreated controls. In the VPA group, transcript levels of *Dpysl4*, *Sox2*, and *Vgf* were significantly decreased compared with the untreated controls on both PND 21 and PND 77 (Table 4). In this group, transcript levels of *Pvalb*, *Snw1*, *Tead3*, and *Wdpcp* were significantly decreased only on PND 21 compared with the untreated controls. In the GLY group, transcript levels of *Acsl4*, *Afdn*, *Arc*, *Arx*, *Baiap2*, *Cxcr4*, *Dgkg*, *Epha5*, *Fgf2*, *Fgf13*, *Gabrb1*, *Grin2b*, *Gsk3b*, *Hes5*, *Kalrn*, *Mas1*, *Neurod2*, *Ptpru*, *Sema3c*, *Snw1*, *Sorl1*, *Stx3*, and *Tcf4* were significantly decreased only on PND 21 compared with the untreated controls (Table 5).

Functional annotation clustering of genes that have been confirmed to show transcript downregulation on PND 21 revealed diverse gene functions by PTU exposure, such as neuron differentiation, regulation of apoptotic process, neuron migration, neurogenesis, neuron projection development, and axon guidance (Table 6). With regard to VPA exposure, finally, selected genes were small in number; however, diverse neural functions were found to be involved, such as neuron differentiation and regulation of neurogenesis (Table 7). Similarly, GLY exposure involved diverse neural functions, such as neuron differentiation, synaptic plasticity, hippocampus development, and neuron migration (Table 8).

4 | DISCUSSION

We have previously found that maternal exposure to PTU, an antithyroid agent that causes hypothyroidism (Shibutani et al., 2009), had diverse effects on hippocampal neurogenesis including aberrations in granule cell lineages, GABAergic interneurons, and synaptic plasticity in rat offspring and that the disruption was mostly sustained through the adult stage on PND 77 (Table 1; Shiraki et al., 2016). However, VPA only affected interneuron subpopulations at the end of maternal

TABLE 4 List of validated genes for transcript-level downregulation on PND 21 and transcript levels of expression on PND 21 and PND 77 after developmental exposure to VPA

Gene	PND 21				PND 77			
	Control		VPA		Control		VPA	
	Normalized by		Normalized by		Normalized by		Normalized by	
	<i>Gapdh</i>	<i>Hprt1</i>	<i>Gapdh</i>	<i>Hprt1</i>	<i>Gapdh</i>	<i>Hprt1</i>	<i>Gapdh</i>	<i>Hprt1</i>
<i>Dpysl4</i>	1.02 \pm 0.19	1.02 \pm 0.24	0.71 \pm 0.14*	1.21 \pm 0.26	1.01 \pm 0.17	1.02 \pm 0.19	0.73 \pm 0.09**	0.67 \pm 0.02**
<i>Sox2</i>	1.04 \pm 0.32	1.04 \pm 0.34	0.53 \pm 0.33*	0.49 \pm 0.31*	1.06 \pm 0.33	1.01 \pm 0.18	0.58 \pm 0.10**	0.54 \pm 0.05**
<i>Vgf</i>	1.00 \pm 0.08	1.01 \pm 0.14	0.86 \pm 0.24	0.75 \pm 0.20*	1.07 \pm 0.35	1.02 \pm 0.21	0.72 \pm 0.18	0.66 \pm 0.12**
<i>Pvalb</i>	1.05 \pm 0.40	1.06 \pm 0.47	0.65 \pm 0.15*	0.65 \pm 0.07	1.03 \pm 0.25	1.00 \pm 0.11	0.94 \pm 0.59	0.85 \pm 0.50
<i>Snw1</i>	1.00 \pm 0.05	1.00 \pm 0.08	0.76 \pm 0.06**	1.28 \pm 0.13**	1.02 \pm 0.20	1.01 \pm 0.17	0.94 \pm 0.17	0.86 \pm 0.08
<i>Tead3</i>	1.02 \pm 0.26	1.01 \pm 0.15	0.80 \pm 0.24	0.79 \pm 0.11*	1.02 \pm 0.21	1.00 \pm 0.06	0.97 \pm 0.28	0.88 \pm 0.22
<i>Wdpcp</i>	1.02 \pm 0.20	1.02 \pm 0.20	0.68 \pm 0.07**	1.16 \pm 0.17	1.03 \pm 0.28	1.01 \pm 0.16	1.03 \pm 0.27	0.93 \pm 0.17

Note. Data are expressed as the mean \pm SD ($n = 6$ /group).

Abbreviations: *Dpysl4*, dihydropyrimidinase-like 4; *Gapdh*, glyceraldehyde-3-phosphate dehydrogenase; *Hprt1*, hypoxanthine phosphoribosyltransferase 1; PND, postnatal day; *Pvalb*, parvalbumin; *Snw1*, SNW domain containing 1; *Sox2*, SRY-box transcription factor 2; *Tead3*, TEA domain transcription factor 3; *Vgf*, VGF nerve growth factor inducible; VPA, valproic acid; *Wdpcp*, WD repeat containing planar cell polarity effector.

* $p < 0.05$ ** $p < 0.01$, significantly different from the untreated controls by Student's or Aspin-Welch's t test.

TABLE 5 List of validated genes for transcript-level downregulation on PND 21 and transcript levels of expression on PND 21 and PND 77 after developmental exposure to GLY

Gene	PND 21				PND 77			
	Control		GLY		Control		GLY	
	Normalized by		Normalized by		Normalized by		Normalized by	
	<i>Gapdh</i>	<i>Hprt1</i>	<i>Gapdh</i>	<i>Hprt1</i>	<i>Gapdh</i>	<i>Hprt1</i>	<i>Gapdh</i>	<i>Hprt1</i>
<i>Acsl4</i>	1.01 ± 0.15	1.01 ± 0.15	0.79 ± 0.25	0.80 ± 0.08*	1.01 ± 0.17	1.00 ± 0.11	0.89 ± 0.07	0.94 ± 0.09
<i>Afdn</i>	1.03 ± 0.27	1.02 ± 0.18	0.68 ± 0.27	0.69 ± 0.16**	1.01 ± 0.17	1.01 ± 0.12	0.93 ± 0.30	0.96 ± 0.24
<i>Arc</i>	1.03 ± 0.27	1.03 ± 0.29	0.37 ± 0.15**	0.42 ± 0.17**	1.12 ± 0.47	1.11 ± 0.45	0.87 ± 0.54	0.92 ± 0.60
<i>Arx</i>	1.05 ± 0.34	1.01 ± 0.14	0.56 ± 0.30*	0.58 ± 0.25**	1.00 ± 0.08	1.01 ± 0.14	0.86 ± 0.34	0.89 ± 0.32
<i>Baiap2</i>	1.03 ± 0.27	1.02 ± 0.22	0.62 ± 0.30*	0.62 ± 0.22*	1.01 ± 0.17	1.01 ± 0.16	0.89 ± 0.22	0.92 ± 0.16
<i>Cxcr4</i>	1.02 ± 0.20	1.03 ± 0.23	0.64 ± 0.25*	1.02 ± 0.28	1.01 ± 0.16	1.00 ± 0.06	0.85 ± 0.17	0.88 ± 0.11
<i>Dgkg</i>	1.08 ± 0.42	1.03 ± 0.27	0.59 ± 0.21*	0.63 ± 0.13**	1.00 ± 0.07	1.00 ± 0.11	0.88 ± 0.22	0.94 ± 0.31
<i>Epha5</i>	1.03 ± 0.27	1.04 ± 0.30	0.64 ± 0.34*	0.55 ± 0.21**	1.02 ± 0.20	1.01 ± 0.14	0.89 ± 0.29	0.92 ± 0.25
<i>Fgf2</i>	1.08 ± 0.48	1.07 ± 0.42	0.53 ± 0.18*	0.54 ± 0.10*	1.10 ± 0.62	1.12 ± 0.71	0.95 ± 0.15	1.01 ± 0.26
<i>Fgf13</i>	1.04 ± 0.33	1.01 ± 0.17	0.60 ± 0.24*	0.65 ± 0.23*	1.01 ± 0.16	1.02 ± 0.23	0.90 ± 0.13	0.95 ± 0.18
<i>Gabrb1</i>	1.01 ± 0.18	1.02 ± 0.20	0.67 ± 0.26*	0.60 ± 0.12**	1.01 ± 0.13	1.01 ± 0.14	0.88 ± 0.14	0.92 ± 0.08
<i>Grin2b</i>	1.02 ± 0.24	1.03 ± 0.25	0.79 ± 0.32	0.71 ± 0.17*	1.01 ± 0.18	1.01 ± 0.16	0.87 ± 0.22	0.91 ± 0.16
<i>Gsk3b</i>	1.00 ± 0.07	1.00 ± 0.07	0.78 ± 0.16*	1.28 ± 0.21	1.00 ± 0.10	1.00 ± 0.06	0.91 ± 0.18	0.95 ± 0.16
<i>Hes5</i>	1.02 ± 0.26	1.02 ± 0.25	0.54 ± 0.17**	0.88 ± 0.15	1.03 ± 0.29	1.02 ± 0.20	0.92 ± 0.18	0.96 ± 0.11
<i>Kalrn</i>	1.06 ± 0.43	1.06 ± 0.41	0.47 ± 0.14*	0.48 ± 0.07*	1.02 ± 0.23	1.02 ± 0.19	0.86 ± 0.11	0.90 ± 0.11
<i>Mas1</i>	1.02 ± 0.23	1.02 ± 0.23	0.68 ± 0.29*	0.70 ± 0.12*	1.01 ± 0.11	1.00 ± 0.03	0.95 ± 0.23	0.99 ± 0.18
<i>Neurod2</i>	1.05 ± 0.35	1.02 ± 0.21	0.55 ± 0.14*	0.62 ± 0.20**	1.01 ± 0.12	1.00 ± 0.05	0.94 ± 0.31	0.96 ± 0.25
<i>Ptpru</i>	1.11 ± 0.57	1.11 ± 0.57	0.43 ± 0.12*	0.69 ± 0.10	1.16 ± 0.53	1.18 ± 0.57	0.81 ± 0.41	0.83 ± 0.37
<i>Sema3c</i>	1.02 ± 0.19	1.01 ± 0.16	0.61 ± 0.23**	0.97 ± 0.25	1.04 ± 0.32	1.02 ± 0.21	0.95 ± 0.23	0.99 ± 0.19
<i>Snw1</i>	1.00 ± 0.05	1.00 ± 0.08	0.83 ± 0.18*	1.35 ± 0.15	1.01 ± 0.12	1.00 ± 0.07	0.96 ± 0.17	1.00 ± 0.11
<i>Sorl1</i>	1.07 ± 0.40	1.03 ± 0.26	0.52 ± 0.22*	0.53 ± 0.10**	1.01 ± 0.15	1.01 ± 0.15	0.99 ± 0.13	1.05 ± 0.17
<i>Stx3</i>	1.01 ± 0.19	1.02 ± 0.21	0.73 ± 0.12*	1.20 ± 0.16	1.01 ± 0.18	1.03 ± 0.24	1.30 ± 0.60	1.36 ± 0.65
<i>Tcf4</i>	1.04 ± 0.31	1.01 ± 0.12	0.67 ± 0.20*	0.75 ± 0.25*	1.00 ± 0.09	1.01 ± 0.12	0.87 ± 0.22	0.91 ± 0.17

Note. Data are expressed as the mean ± SD ($n = 6$ /group).

Abbreviations: *Acsl4*, acyl-CoA synthetase long-chain family member 4; *Afdn*, afadin, adherens junction formation factor; *Arc*, activity-regulated cytoskeleton-associated protein; *Arx*, aristaless-related homeobox; *Baiap2*, BAR/IMD domain containing adaptor protein 2; *Cxcr4*, C-X-C motif chemokine receptor 4; *Dgkg*, diacylglycerol kinase, gamma; *Epha5*, EPH receptor A5; *Fgf2*, fibroblast growth factor 2; *Fgf13*, fibroblast growth factor 13; *Gabrb1*, gamma-aminobutyric acid type A receptor subunit beta1; *Gapdh*, glyceraldehyde-3-phosphate dehydrogenase; GLY, glycidol; *Grin2b*, glutamate ionotropic receptor NMDA type subunit 2B; *Gsk3b*, glycogen synthase kinase 3 beta; *Hes5*, hes family bHLH transcription factor 5; *Hprt1*, hypoxanthine phosphoribosyltransferase 1; *Kalrn*, kalirin, RhoGEF kinase; *Mas1*, MAS1 proto-oncogene, G protein-coupled receptor; *Neurod2*, neuronal differentiation 2; PND, postnatal day; *Ptpru*, protein tyrosine phosphatase, receptor type, U; *Sema3c*, semaphorin 3C; *Snw1*, SNW domain containing 1; *Sorl1*, sortilin-related receptor 1; *Stx3*, syntaxin 3; *Tcf4*, transcription factor 4.

* $p < 0.05$. ** $p < 0.01$, significantly different from the untreated controls by Student's or Aspin-Welch's t test.

exposure and typically showed a late effect on granule cell lineages involving synaptic plasticity at the adult stage (Table 1; Watanabe et al., 2017). GLY had a reversible effect on granule cell lineages at the end of maternal exposure and a sustained effect on interneuron subpopulations (Table 1; Akane, Shiraki et al., 2013). However, in nature, the effect on interneurons may be transient and disappear later on, because the change in granule cell lineages disappeared along with a compensatory increase in synaptic plasticity at the adult stage (Table 1; Akane, Shiraki et al., 2013, Akane et al., 2014). In the present study, validation analysis of transcript levels of selected genes confirmed the downregulation of many genes on PND 21 induced by exposure to

PTU or GLY, reflecting the diverse effects on neurogenesis by these compounds. Furthermore, genes showing sustained downregulation were found with PTU or VPA exposure, reflecting sustained or late effect on neurogenesis by these compounds. VPA is a HDAC inhibitor, which may cause suppression of DNA methylation, because HDAC activation and DNA methylation usually cooperate in transcriptional gene silencing (Sasidharan Nair et al., 2020). This may be the reason for the lower number of validated genes showing transcript downregulation on PND 21 with VPA compared with PTU and GLY. In contrast, GLY did not induce sustained downregulation, probably because of the reversible nature of its effect on neurogenesis.

TABLE 6 Classification of hypermethylated and downregulated genes by means of functional annotation clustering in the hippocampal dentate gyrus of offspring on PND 21 after maternal exposure to PTU

Gene function	Number of genes	Gene symbol
Neuron differentiation	15	<i>Cebpb</i> ^a , <i>Hes5</i> ^a , <i>Acsl4</i> , <i>Arhgef2</i> , <i>Atp2b2</i> , <i>Baiap2</i> , <i>Id2</i> , <i>Neurod6</i> , <i>Ptpru</i> , <i>Shh</i> , <i>Tfap2c</i> , <i>Wnt7b</i> , <i>Wnt8b</i> , <i>Wnt9a</i> , <i>Wnt16</i>
Apoptotic process	11	<i>Bmp3</i> ^a , <i>Cebpb</i> ^a , <i>Creb1</i> ^a , <i>Epha7</i> ^a , <i>Fgf13</i> ^a , <i>Fzd9</i> ^a , <i>Arhgef2</i> , <i>Dab2ip</i> , <i>Igf1</i> , <i>Six4</i> , <i>Vegfa</i>
Neuron migration	8	<i>Fgf13</i> ^a , <i>Reln</i> ^a , <i>Sema3c</i> ^a , <i>Arhgef2</i> , <i>Cntn2</i> , <i>Dab2ip</i> , <i>Ndel1</i> , <i>Robo3</i>
Neurogenesis	6	<i>Hes5</i> ^a , <i>Arhgef2</i> , <i>Dll4</i> , <i>Numbl</i> , <i>Thrsp</i> , <i>Wnt7b</i>
Neuron projection development	6	<i>Reln</i> ^a , <i>Baiap2</i> , <i>Cntn2</i> , <i>Dab2ip</i> , <i>Ndel1</i> , <i>Wnt7b</i>
Axon guidance	5	<i>Reln</i> ^a , <i>Epha5</i> , <i>Robo3</i> , <i>Sema3c</i> ^a , <i>Vegfa</i>
Hippocampus development	4	<i>Fgf13</i> ^a , <i>Mas1</i> ^a , <i>Reln</i> ^a , <i>Epha5</i>
Neuroblast proliferation	4	<i>Fzd9</i> ^a , <i>Numbl</i> , <i>Shh</i> , <i>Vegfa</i>
Synaptic plasticity	4	<i>Arc</i> ^a , <i>Atp2b2</i> , <i>Baiap2</i> , <i>Cntn2</i>
Axonogenesis	4	<i>Creb1</i> ^a , <i>Cntn2</i> , <i>Ndel1</i> , <i>Numbl</i>
Astrocyte differentiation, astrocyte development	4	<i>Hes5</i> ^a , <i>Cntn2</i> , <i>Id2</i> , <i>Ror2</i>
Oligodendrocyte differentiation, oligodendrocyte development, and myelination	4	<i>Hes5</i> ^a , <i>Cntn2</i> , <i>Id2</i> , <i>Shh</i>
Neural precursor cell proliferation	3	<i>Fzd9</i> ^a , <i>Dll4</i> , <i>Id2</i>
Glial cell differentiation	3	<i>Reln</i> ^a , <i>Fgf2</i> , <i>Igf1</i>
Dendrite development	2	<i>Baiap2</i> , <i>Dab2ip</i>
Ephrin signaling pathway	2	<i>Epha7</i> ^a , <i>Epha5</i>
Regulation of cytosolic calcium ion concentration	2	<i>Pvalb</i> ^a , <i>Atp2b2</i>
Synaptic transmission, glutamatergic	2	<i>Reln</i> ^a , <i>Ror2</i>
Neuronal stem cell population maintenance	1	<i>Hes5</i> ^a
Radial glial cell differentiation	1	<i>Hes5</i> ^a
Establishment of neuroblast polarity	1	<i>Fgf13</i> ^a
Asymmetric neuroblast division	1	<i>Arhgef2</i>
Cerebral cortex GABAergic interneuron migration	1	<i>Cntn2</i>
Dopamine biosynthetic process	1	<i>Dao</i>

Abbreviations: *Acsl4*, acyl-CoA synthetase long-chain family member 4; *Arc*, activity-regulated cytoskeleton-associated protein; *Arhgef2*, Rho guanine nucleotide exchange factor 2; *Atp2b2*, ATPase plasma membrane Ca²⁺ transporting 2; *Baiap2*, BAR/IMD domain containing adaptor protein 2; *Bmp3*, bone morphogenetic protein 3; *Cebpb*, CCAAT/enhancer-binding protein beta; *Cntn2*, contactin 2; *Creb1*, cAMP-responsive element-binding protein 1; *Dab2ip*, DAB2-interacting protein; *Dao*, D-amino-acid oxidase; *Dll4*, delta-like canonical Notch ligand 4; *Epha5*, EPH receptor A5; *Epha7*, Eph receptor A7; *Fgf2*, fibroblast growth factor 2; *Fgf13*, fibroblast growth factor 13; *Fzd9*, frizzled class receptor 9; *Gapdh*, glyceraldehyde-3-phosphate dehydrogenase; *Hes5*, hes family bHLH transcription factor 5; *Hprt1*, hypoxanthine phosphoribosyltransferase 1; *Id2*, inhibitor of DNA-binding 2; *Igf1*, insulin-like growth factor 1; *Mas1*, MAS1 proto-oncogene, G protein-coupled receptor; *Ndel1*, nudE neurodevelopment protein 1-like 1; *Neurod6*, neuronal differentiation 6; *Numbl*, NUMB-like, endocytic adaptor protein; PND, postnatal day; *Ptpru*, protein tyrosine phosphatase, receptor type, U; PTU, 6-propyl-2-thiouracil; *Pvalb*, parvalbumin; *Reln*, reelin; *Robo3*, roundabout guidance receptor 3; *Ror2*, receptor tyrosine kinase-like orphan receptor 2; *Sema3c*, semaphorin 3C; *Shh*, sonic hedgehog signaling molecule; *Six4*, SIX homeobox 4; *Tfap2c*, transcription factor AP-2 gamma; *Thrsp*, thyroid hormone responsive; *Vegfa*, vascular endothelial growth factor A; *Wnt7b*, Wnt family member 7B; *Wnt8b*, Wnt family member 8B; *Wnt9a*, Wnt family member 9A; *Wnt16*, Wnt family member 16.

^aDownregulated on both PND 21 and PND 77.

In the present study, PTU downregulated *Creb1* on both PND 21 and PND 77. The translated product, cAMP-responsive element-binding protein (CREB), is a transcription factor in the nervous system

that is involved in diverse processes such as neurodevelopment, synaptic plasticity, and neuroprotection (Sakamoto et al., 2011). The irreversible reduction in CREB protein was observed in the dentate gyrus,

TABLE 7 Classification of hypermethylated and downregulated genes by means of functional annotation clustering in the hippocampal dentate gyrus of offspring on PND 21 after maternal exposure to VPA

Gene function	Number of genes	Gene symbol
Neuron differentiation	2	<i>Sox2^a</i> , <i>Vgf^a</i>
Regulation of neurogenesis	2	<i>Sox2^a</i> , <i>Snw1</i>
Neuronal stem cell population maintenance	1	<i>Tead3</i>
Asymmetric neuroblast division	1	<i>Tead3</i>
Neuroblast proliferation	1	<i>Sox2^a</i>
Neuron projection guidance	1	<i>Dpysl4^a</i>
Synaptic plasticity	1	<i>Vgf^a</i>
Regulation of cytosolic calcium ion concentration	1	<i>Pvalb</i>
Nervous system development	1	<i>Wdpcp</i>

Abbreviations: *Dpysl4*, dihydropyrimidinase-like 4; *Gapdh*, glyceraldehyde-3-phosphate dehydrogenase; *Hprt1*, hypoxanthine phosphoribosyltransferase 1; PND, postnatal day; *Pvalb*, parvalbumin; *Snw1*, SNW domain containing 1; *Sox2*, SRY-box transcription factor 2; *Tead3*, TEA domain transcription factor 3; *Vgf*, VGF nerve growth factor inducible; VPA, valproic acid; *Wdpcp*, WD repeat containing planar cell polarity effector.

^aDownregulated on both PND 21 and PND 77.

cornu Ammonis (CA) 1, and CA3 of the hippocampus in rats after maternal PTU exposure (Dong et al., 2009). Reduction in the expression of CREB or in the active phosphorylated CREB was also observed in the hippocampus in rat offspring after maternal thyroidectomy (Zhang et al., 2015). CREB is closely related in structure and function to cAMP-response element modulator (CREM), and mice with a *Crem*^{-/-} background and lacking CREB in the brain during prenatal life show extensive apoptosis of postmitotic neurons (Mantamadiotis et al., 2002), as well as delayed migration of neural and glial progenitors (Díaz-Ruiz et al., 2008). By contrast, mice in which both *Creb1* and *Crem* are disrupted in the postnatal forebrain show progressive neuronal loss (Mantamadiotis et al., 2002). Maternal PTU exposure in our previous study induced reductions in NSCs and neural progenitor cells by apoptosis at the end of exposure and sustained reduction in early progenitor cells later on (Table 1; Shiraki et al., 2016). However, the number of postmitotic immature granule cells was unaffected. Moreover, developmental hypothyroidism, such as that induced by PTU exposure, causes neuronal mismigration in the hippocampus (Shibutani et al., 2009), suggesting involvement of CREB/CREM downregulation in the neuronal mismigration. Although data are not included in the list of selected genes, we found PTU exposure caused promoter region hypermethylation and downregulation of transcript level of *Crem* by analysis of Methyl-Seq and RNA-Seq, respectively.

CREB also plays a role in synaptic plasticity and acts as a transcription factor of immediate-early genes (IEGs) related to synaptic plasticity (Kaldun & Sprecher, 2019). *Arc* is one of these target IEGs; we observed a decrease in activity-regulated cytoskeleton-associated protein (ARC)⁺ granule cells at the end of maternal PTU exposure on PND 21, suggestive of suppressed synaptic plasticity (Table 1; Shiraki et al., 2016). In the present study, *Arc* was hypermethylated on PND 21 and downregulated on both PND 21 and PND 77 due to maternal PTU exposure. These results suggest the involvement of multiple mechanisms in the transcriptional suppression of *Arc*.

In the current study, PTU downregulated *Hes5* on both PND 21 and PND 77. The translated product, hes family bHLH transcription factor 5 (HES5), is expressed in NSCs to suppress the transcription and function of activator-type bHLH factor as an effector of the Notch signal, and thus maintains NSCs and early progenitor cells (Lugert et al. 2010). Notch activation-mediated promotion of hippocampal neurogenesis involves the activation of downstream molecules, such as CREB (Baik et al., 2020). As aforementioned, PTU in this study caused sustained *Creb1* downregulation. Therefore, it is reasonable to consider that PTU-mediated developmental hypothyroidism causes suppression of Notch signaling through downregulation of HES5 and CREB1, resulting in decreased numbers of NSCs and early progenitor cells on PND 21 and a sustained decrease in early progenitor cells on PND 77 as observed in our previous study (Table 1; Shiraki et al., 2016).

Herein, PTU downregulated *Tfap2c* on PND 21. Transcription factor AP-2 gamma (TFAP2C) is expressed in type-2b and -3 neural progenitor cells in the hippocampal dentate gyrus and plays a role in promoting proliferation and differentiation to produce postmitotic granule cells (Mateus-Pinheiro et al., 2017). Maternal PTU exposure in our previous study caused reductions in type-1 NSCs and type-2a and type-3 progenitor cells in the SGZ on PND 21 (Table 1; Shiraki et al., 2016), suggesting that *Tfap2c* downregulation reflects the reduction in type-3 progenitor cells at this time point.

In the present study, PTU also downregulated *Robo3* on PND 21, which is consistent with our previous expression microarray data (Shiraki et al., 2014). Roundabout guidance receptor 3 (ROBO3) and its ligand, neural EGFL-like 2, regulate axon guidance, and neuronal migration in the developing brain (Pak et al., 2020). Furthermore, PTU downregulated *Sema3c* on both PND 21 and PND 77 in this study, and this result was consistent with our previous expression microarray data on PND 21 (Shiraki et al., 2014). Semaphorins and their receptors, neuropilins, are expressed in the developing hippocampus and

TABLE 8 Classification of hypermethylated and downregulated genes by means of functional annotation clustering in the hippocampal dentate gyrus of offspring on PND 21 after maternal exposure to GLY

Gene function	Number of genes	Gene symbol
Neuron differentiation	7	<i>Acsl4, Baiap2, Gsk3b, Hes5, Neurod2, Ptpru, Tcf4</i>
Synaptic plasticity	6	<i>Arc, Baiap2, Grin2b, Gsk3b, Kalrn, Neurod2</i>
Hippocampus development	5	<i>Epha5, Fgf13, Grin2b, Gsk3b, Mas1</i>
Neuron migration	5	<i>Arx, Cxcr4, Fgf13, Gsk3b, Sema3c</i>
Axon guidance	3	<i>Arx, Epha5, Sema3c</i>
Neuron projection development	3	<i>Baiap2, Gsk3b, Stx3</i>
Dendrite development	3	<i>Baiap2, Gsk3b, Kalrn</i>
Oligodendrocyte differentiation, oligodendrocyte development, and myelination	3	<i>Afdn, Cxcr4, Hes5</i>
Neuron development	3	<i>Dgkg, Epha5, Gabrb1</i>
Neurogenesis	2	<i>Cxcr4, Hes5, Snw1, Sorl1</i>
Radial glial cell differentiation	2	<i>Afdn, Hes5</i>
Apoptotic process	2	<i>Fgf13, Gsk3b</i>
Axonogenesis	2	<i>Gsk3b, Kalrn</i>
Neuronal stem cell population maintenance	1	<i>Hes5</i>
Establishment of neuroblast polarity	1	<i>Fgf13</i>
Neural precursor cell proliferation	1	<i>Cxcr4</i>
Neuron maturation	1	<i>Gsk3b</i>
Cerebral cortex GABAergic interneuron migration	1	<i>Arx</i>
Glial cell differentiation	1	<i>Fgf2</i>
Astrocyte differentiation	1	<i>Hes5</i>
Ephrin signaling pathway	1	<i>Epha5</i>

Abbreviations: *Acsl4*, acyl-CoA synthetase long-chain family member 4; *Afdn*, afadin, adherens junction formation factor; *Arc*, activity-regulated cytoskeleton-associated protein; *Arx*, aristaless-related homeobox; *Baiap2*, BAR/IMD domain containing adaptor protein 2; *Cxcr4*, C-X-C motif chemokine receptor 4; *Dgkg*, diacylglycerol kinase, gamma; *Epha5*, EPH receptor A5; *Fgf2*, fibroblast growth factor 2; *Fgf13*, fibroblast growth factor 13; *Gabrb1*, gamma-aminobutyric acid type A receptor subunit beta1; *Gapdh*, glyceraldehyde-3-phosphate dehydrogenase; GLY, glycidol; *Grin2b*, glutamate ionotropic receptor NMDA type subunit 2B; *Gsk3b*, glycogen synthase kinase 3 beta; *Hes5*, hes family bHLH transcription factor 5; *Hprt1*, hypoxanthine phosphoribosyltransferase 1; *Kalrn*, kalirin, RhoGEF kinase; *Mas1*, MAS1 proto-oncogene, G protein-coupled receptor; *Neurod2*, neuronal differentiation 2; PND, postnatal day; *Ptpru*, protein tyrosine phosphatase, receptor type, U; *Sema3c*, semaphorin 3C; *Snw1*, SNW domain containing 1; *Sorl1*, sortilin-related receptor 1; *Stx3*, syntaxin 3; *Tcf4*, transcription factor 4.

are associated with axon tract and synapse formation through cytoskeleton reorganization of the axonal growth cone (Gil and Del Río, 2019). In the developing brain, semaphorin 3C (SEMA3C) was found to be a critical component required for radial migration of developing neurons (Wiegrefe et al., 2015). These results suggest an involvement of ROBO3 or SEMA3C downregulation in the neuronal mismigration and axon guidance induced by developmental hypothyroidism, as well as the involvement of CREB/CREM downregulation as aforementioned.

In our study, PTU downregulated *Epha7* on both PND 21 and PND 77 and *Epha5* on PND 21. The promoter region hypermethylation and downregulation of transcript level have already been reported for *Epha5* in rats with developmental hypothyroidism (Wu et al., 2015). In our previous microarray analysis, maternal PTU

exposure caused downregulation of *Epha4*, *Epha6*, *Epha8*, *Ephb2*, and *Ephb6* in the hippocampal dentate gyrus (Shiraki et al., 2014), as well as a decrease in Eph receptor A4 (EPHA4)⁺ cells in the hilus of the dentate gyrus (Table 1; Shiraki et al., 2016). *Epha* receptors and ephrin-A ligands play important roles in neural development and synaptic plasticity, and among them, EPHA7 gene mutations have been reported to be linked to developmental neurological delays (Wurzman et al., 2015). EPHA7 is required for connectivity stabilization of parvalbumin (PVALB)-expressing GABAergic interneurons with granule cells of the dentate gyrus (Beuter et al., 2016). We have previously found that maternal PTU exposure caused a sustained decrease in PVALB⁺ interneurons in the hilus of the dentate gyrus (Table 1; Shiraki et al., 2016), suggesting a causal relationship of sustained *Epha7* downregulation with the decrease in PVALB⁺ interneurons.

With regard to EPHA5, binding of ephrin-A5 to this receptor activates the CREB signal transduction pathway to induce spine maturation and filopodia formation in synaptogenesis (Akaneya et al., 2010). As aforementioned, the present study also revealed the downregulation of *Creb1* and *Epha5* by PTU on PND 21, suggesting suppression of the signaling cascade in synaptic plasticity, as evident by the decrease in ARC⁺ granule cells at this time point (Table 1; Shiraki et al., 2016).

PTU also downregulated *Pvalb* on both PND 21 and PND 77, in accordance with the decrease in PVALB⁺ interneurons as aforementioned (Table 1; Shiraki et al., 2016). We have also previously reported promoter region hypermethylation and downregulation of *Pvalb*, accompanying reduction in PVALB⁺ interneurons in the dentate gyrus upon maternal manganese exposure in mice (Wang et al., 2013). GABAergic interneurons that promote differentiation of intermediate progenitor populations are considered to be basket cells or axo-axonic cells (Tozuka et al., 2005). Considering that subpopulations of basket cells or axo-axonic cells express PVALB (Freund and Buzsáki, 1996), reduction in PVALB⁺ interneurons by maternal PTU exposure may also be caused by promoter region hypermethylation, leading to the reduction in type-3 progenitor cells (Table 1; Shiraki et al., 2016).

In the present study, PTU downregulated *Reln* on both PND 21 and PND 77. However, this result was in contrast to the *Reln* upregulation and increase in reelin (RELN)⁺ interneurons induced by maternal PTU exposure in our previous study (Table 1; Shiraki et al., 2016). Although the reason for this discrepancy is not clear, there is a report that showed promoter region hypermethylation and downregulation of transcript level of *Reln* at early PNDs in pups exposed to PTU from GD 15 to weaning; however, this change gradually disappeared after PND 15 (Sui & Li, 2010). After weaning, the increase in RELN⁺ interneurons in our previous study is thought to be a compensatory response against neuronal mismigration.

Herein, on PND 21 PTU downregulated *Hes5*, *Cntn2*, *Id2*, and *Shh*, which are associated with oligodendrocyte development and differentiation, and myelination, as well as *Hes5*, *Cntn2*, *Id2*, and *Ror2*, which are associated with astrocyte development and differentiation, and finally *Reln*, *Fgf2*, and *Igf*, which are associated with glial cell differentiation. We have previously reported that developmental hypothyroidism causes increases in immature astrocytes immunoreactive for vimentin and glial fibrillary acidic protein in the cerebral white matter, as well as decreases in oligodendrocytes immunoreactive for 2',3'-cyclic nucleotide 3'-phosphodiesterase or oligodendrocyte lineage transcription factor 2 in several brain regions (Shibutani et al., 2009; Shiraki et al., 2014). The differentiation of oligodendrocytes is strongly thyroid hormone-dependent (Rodríguez-Peña, 1999). Delivery of sonic hedgehog signaling molecule (SHH) into demyelinated lesions in rats following spinal cord injury increased oligodendrocyte precursors and neurons (Bambakidis et al., 2003), suggesting that a decrease in oligodendrocytes due to developmental hypothyroidism may be mediated by SHH downregulation.

The VPA-induced autism model, as well as other autism models, has shown alterations in GABAergic signals, as evident by reductions in glutamate decarboxylase 67 (GAD67)⁺ and PVALB⁺ interneuron subpopulations in the cerebral cortex (Cellot and Cherubini, 2014).

We have also previously found decreases in RELN⁺, PVALB⁺, or GAD67⁺ interneurons on PND 21 induced by maternal VPA exposure (Table 1; Watanabe et al., 2017). In the present study, we found DNA hypermethylation and downregulation in the transcript level of *Pvalb* at the same time point, suggesting the involvement of epigenetic gene regulation in disruptive regulation of GABAergic signals during hippocampal neurogenesis.

VPA also downregulated *Vgf* and *Dpysl4* on PND 21 and PND 77. TLQP-62, a VGF-derived peptide, has been shown to enhance dendritic maturation in the rat hippocampus (Behnke et al., 2017) and induce neuritogenesis in human SH-SY5Y neuroblastoma-derived cell line (Moutinho et al., 2020). Dihydropyrimidinase-like 4 is highly expressed in the hippocampus from early postnatal development, playing critical roles in both axonal and dendritic morphogenesis of dentate granule cells (Quach et al., 2018). Therefore, *Vgf* and *Dpysl4* downregulation may suppress synaptic plasticity in the hippocampal dentate gyrus. However, we have previously revealed that VPA exposure increased ARC or cyclooxygenase 2-mediated synaptic plasticity as a late effect at the adult stage (Table 1; Watanabe et al., 2017). Although we did not examine microRNA expression, microRNA-mediated homeostatic synaptic plasticity can be induced as a compensatory response to alterations in neuronal activity (Hou et al., 2015).

We have previously reported that maternal GLY exposure decreased immature granule cells in the dentate gyrus and increased GABAergic interneuron subpopulations as represented by immature RELN⁺ interneurons and calretinin⁺ interneurons in the hilus on PND 21 (Table 1; Akane, Shiraki et al., 2013). The increases in immature RELN⁺ interneurons remained until PND 77, although the change in granule cell lineage disappeared (Akane, Shiraki et al., 2013). We have also found that GLY causes axon injury in the central and peripheral nervous systems of adult rats (Akane, Shiraki et al., 2013). In accordance with our previous results, GLY exposure downregulated the transcript levels of genes involved in neuronal migration (*Arx*, *Cxcr4*, *Fgf13*, *Gsk3b*, and *Sema3c*), neuron projection development (*Baiap2*, *Gsk3b*, and *Stx3*), dendrite development (*Baiap2*, *Gsk3b*, and *Kalrn*), and axonogenesis (*Gsk3b* and *Kalrn*) on PND 21. However, the expression of all the downregulated genes recovered on PND 77. These gene expression changes may support suppressed differentiation and mismigration of late-stage hippocampal neurogenesis at the end of GLY exposure, targeting the newly generated nerve terminals of immature granule cells (Akane, Shiraki et al., 2013).

Herein, GLY downregulated the transcript levels of genes involved in synaptic plasticity (*Arc*, *Baiap2*, *Grin2b*, *Gsl3b*, *Kalrn*, and *Neurod2*) on PND 21, probably reflecting toxicity to newly generating nerve terminals of immature granule cells (Table 1; Akane, Shiraki et al., 2013). On PND 77 after maternal GLY exposure, we have previously found an increase in ARC⁺ and FBJ osteosarcoma oncogene (FOS)⁺ hippocampal granule cells (Table 1; Akane et al., 2014). As well as ARC, FOS is an IEG protein regulating synaptic plasticity (Minatohara et al. 2016), and these late responses may be the result of amelioration from disruption of late-stage differentiation in hippocampal neurogenesis.

In the present study, 10 genes showed downregulation in the transcript level on PND 21 in common with both PTU and GLY. Among them, five genes showed sustained downregulation through PND 77 only in the PTU group. However, we could not find any genes that showed sustained downregulation through PND 77 in the GLY group. There may be two possibilities on the difference in the response of mRNA expression on PND 77. As one possibility, GLY-exposed animals allowed active demethylation of methylated cytosine in hypermethylated genes. Another possibility is that the methylation pattern of promoter region is different between the PTU and GLY groups. In the present study, we selected genes that showed CpG site hypermethylation with the ratio of ≥ 0.2 as compared with the untreated controls on PND 21. Among the five genes showing sustained downregulation by PTU, *Fgf13* and *Mas1* differed the methylated CpG sites between PTU and GLY (Tables S6 and S8), and this difference may cause different responses in transcription on PND 77 between PTU and GLY. In contrast, three other genes, *Arc*, *Hes5*, and *Sema3C*, showed methylation of identical CpG sites with both PTU and GLY (Tables S6 and S8). However, methylation ratios of the corresponding and nearby CpG sites in the promoter region of these genes were higher with PTU as compared with GLY (Tables S6 and S8). It may be possible that the relatively high methylation ratios of the promoter region cause sustained suppression of transcription of these genes through PND 77. Further studies addressing the stability of promoter region hypermethylation of the identified genes, as well as the relationship with gene expression changes, may be necessary for establishing irreversible markers of DNT.

In the present study, maternal food and water consumption were decreased by exposure to PTU, VPA, or GLY. Offspring of these exposure groups, especially of PTU and GLY, decreased the body weight until PND 77. These results suggest treatment-derived undernutrition and stress on both dams and offspring. Nutrients involved in one-carbon metabolism, such as methionine, choline, and folic acid, work as methyl donors for maintaining gDNA methylation (Friso and Choi, 2002). Experimentally, prenatal and/or postnatal nutritional deficiency, as well as prenatal or early-life postnatal stress, has shown to cause alterations in the methylation status of both genome-wide and specific gene levels in several brain regions in mice and rats (Weng et al., 2014; Xu et al., 2014; Blaze & Roth, 2015). Among the genes identified as hypermethylated ones in the present study, *Reln* has previously shown to be examined the methylation status in brain regions. In one study, early-life postnatal stress caused *Reln* hypomethylation in the hippocampus of rats (Wang et al., 2018). In contrast, prenatal dietary methyl donor deficiency did not alter the methylation level of *Reln*, in contrast to the hypermethylation of *Nnat* encoding neuronatin, in the hippocampus of rats (Konycheva et al., 2011). On the other hand, prenatal stress caused hypermethylation of *Reln*, as well as *Gad1* encoding GAD67 and *Bdnf* encoding brain-derived neurotrophic factor, in the frontal cortex by prenatal stress in mice (Dong et al., 2016). These results may suggest possible modifying effects in the methylation status of genes identified as hypermethylated ones in exposure groups especially of PTU and GLY in the present study.

In conclusion, PTU and GLY confirmed the downregulation of many genes on PND 21, reflecting their diverse effects on neurogenesis. Furthermore, genes showing sustained downregulation were found upon PTU and VPA exposure, reflecting sustained or late effect on neurogenesis by these compounds. In contrast, these effects were not observed with GLY, probably because of the reversible nature of the effects. Among the genes showing sustained downregulation, *Creb*, *Arc*, and *Hes5* were concurrently downregulated by PTU, suggestive of an association with neuronal migration, suppressed synaptic plasticity, and reduced neural stem and progenitor cells. *Epha7* and *Pvalb* were also concurrently downregulated by PTU, suggestive of an association with the reduction in late-stage progenitor cells. VPA induced sustained downregulation of *Vgf* and *Dpysl4*, which may be related to aberrations in synaptic plasticity. The genes that showed sustained downregulation, that is, *Arc*, *Bmp3*, *Cebpb*, *Creb1*, *Epha7*, *Fgf13*, *Fzd9*, *Hes5*, *Mas1*, *Pvalb*, *Reln*, *Sema3c*, *Dpysl4*, *Sox2*, and *Vgf*, may be markers of irreversible DNT.

ACKNOWLEDGEMENTS

The authors thank Yayoi Khono for her technical assistance in preparing the histological specimens. This work was supported by Grant-in-Aid for Scientific Research (B) from the Japan Society for the Promotion of Science (JSPS; Grant 18H02341). We thank Michal Bell, PhD, from Edanz Group (<https://en-author-services.edanzgroup.com/ac>) for editing a draft of this manuscript.

CONFLICT OF INTEREST

All authors declare that there are no conflicts of interest that influenced the outcome of the present study.

ORCID

Makoto Shibutani  <https://orcid.org/0000-0003-3417-9697>

REFERENCES

- Akane, H., Saito, F., Shiraki, A., Takeyoshi, M., Imatanaka, N., Itahashi, M., ... Shibutani, M. (2014). Downregulation of immediate-early genes linking to suppression of neuronal plasticity in rats after 28-day exposure to glycidol. *Toxicology and Applied Pharmacology*, 279(2), 150–162. <https://doi.org/10.1016/j.taap.2014.05.017>
- Akane, H., Saito, F., Yamanaka, H., Shiraki, A., Imatanaka, N., Akahori, Y., ... Shibutani, M. (2013). Methacarn as a whole brain fixative for gene and protein expression analyses of specific brain regions in rats. *Journal of Toxicological Sciences*, 38(3), 431–443. <https://doi.org/10.2131/jts.38.431>
- Akane, H., Shiraki, A., Imatanaka, N., Akahori, Y., Itahashi, M., Ohishi, T., ... Shibutani, M. (2013). Glycidol induces axonopathy by adult-stage exposure and aberration of hippocampal neurogenesis affecting late-stage differentiation by developmental exposure in rats. *Toxicological Sciences*, 134(1), 140–154. <https://doi.org/10.1093/toxsci/kft092>
- Akane, Y., Sohya, K., Kitamura, A., Kimura, F., Washburn, C., Zhou, R., ... Ziff, E. B. (2010). Ephrin-A5 and EphA5 interaction induces synaptogenesis during early hippocampal development. *PLoS ONE*, 5(8), e12486. <https://doi.org/10.1371/journal.pone.0012486>
- Baik, S. H., Rajeev, V., Fann, D. Y., Jo, D. G., & Arumugam, T. V. (2020). Intermittent fasting increases adult hippocampal neurogenesis. *Brain and Behavior*, 10(1), e01444. <https://doi.org/10.1002/brb3.1444>

- Bambakidis, N. C., Wang, R. Z., Franic, L., & Miller, R. H. (2003). Sonic hedgehog-induced neural precursor proliferation after adult rodent spinal cord injury. *Journal of Neurosurgery*, 99(1 Suppl), 70–75. <https://doi.org/10.3171/spi.2003.99.1.0070>
- Behnke, J., Cheedalla, A., Bhatt, V., Bhat, M., Teng, S., Palmieri, A., ... Alder, J. (2017). Neuropeptide VGF promotes maturation of hippocampal dendrites that is reduced by single nucleotide polymorphisms. *International Journal of Molecular Sciences*, 18(3), 612. <https://doi.org/10.1016/j.ijms.2015.04.004>
- Beuter, S., Ardi, Z., Horovitz, O., Wuchter, J., Keller, S., Saha, R., ... Volkmer, H. (2016). Receptor tyrosine kinase EphA7 is required for interneuron connectivity at specific subcellular compartments of granule cells. *Scientific Reports*, 6, 29710. <https://doi.org/10.1038/srep29710>
- Blaze, J., & Roth, T. L. (2015). Evidence from clinical and animal model studies of the long-term and transgenerational impact of stress on DNA methylation. *Seminars in Cell & Developmental Biology*, 43, 76–84. <https://doi.org/10.1016/j.semcd.2015.04.004>
- Cameron, H. A., McEwen, B. S., & Gould, E. (1995). Regulation of adult neurogenesis by excitatory input and NMDA receptor activation in the dentate gyrus. *Journal of Neuroscience*, 15(6), 4687–4692. <https://doi.org/10.1523/JNEUROSCI.15-06-04687.1995>
- Ceccatelli, S., Bose, R., Edoff, K., Onishchenko, N., & Spulber, S. (2013). Long-lasting neurotoxic effects of exposure to methylmercury during development. *Journal of Internal Medicine*, 273(5), 490–497. <https://doi.org/10.1111/joim.12045>
- Cellot, G., & Cherubini, E. (2014). GABAergic signaling as therapeutic target for autism spectrum disorders. *Frontiers in Pediatrics*, 2, 70. <https://doi.org/10.3389/fped.2014.00070>
- Covic, M., Karaca, E., & Lie, D. C. (2010). Epigenetic regulation of neurogenesis in the adult hippocampus. *Heredity*, 105(1), 122–134. <https://doi.org/10.1038/hdy.2010.27>
- Díaz-Ruiz, C., Parlato, R., Aguado, F., Ureña, J. M., Burgaya, F., Martínez, A., ... Soriano, E. (2008). Regulation of neural migration by the CREB/CREM transcription factors and altered Dab1 levels in CREB/CREM mutants. *Molecular and Cellular Neurosciences*, 39(4), 519–528. <https://doi.org/10.1016/j.mcn.2008.07.019>
- Dong, E., Tueting, P., Matrisciano, F., Grayson, D. R., & Guidotti, A. (2016). Behavioral and molecular neuroepigenetic alterations in prenatally stressed mice: Relevance for the study of chromatin remodeling properties of antipsychotic drugs. *Translational Psychiatry*, 6(1), e711. <https://doi.org/10.1038/tp.2015.191>
- Dong, J., Liu, W., Wang, Y., Hou, Y., Xi, Q., & Chen, J. (2009). Developmental iodine deficiency resulting in hypothyroidism reduces hippocampal ERK1/2 and CREB in lactational and adolescent rats. *BMC Neuroscience*, 10, 149. <https://doi.org/10.1186/1471-2202-10-149>
- Fonnum, F., Karlsen, R. L., Malthe-Sørensen, D., Skrede, K. K., & Walaas, I. (1979). Localization of neurotransmitters, particularly glutamate, in hippocampus, septum, nucleus accumbens and superior colliculus. *Progress in Brain Research*, 51, 167–191. [https://doi.org/10.1016/S0079-6123\(08\)61304-7](https://doi.org/10.1016/S0079-6123(08)61304-7)
- Freund, T. F., & Buzsáki, G. (1996). Interneurons of the hippocampus. *Hippocampus*, 6, 347–470. [https://doi.org/10.1002/\(SICI\)1098-1063\(1996\)6:4<347::AID-HIPO1>3.0.CO;2-I](https://doi.org/10.1002/(SICI)1098-1063(1996)6:4<347::AID-HIPO1>3.0.CO;2-I)
- Friso, S., & Choi, S. (2002). Gene-nutrient interactions and DNA methylation. *The Journal of Nutrition*, 132(8 Suppl), 2382S–2387S. <https://doi.org/10.1093/jn/132.8.2382S>
- Gil, V., & Del Río, J. A. (2019). Functions of plexins/neuropilins and their ligands during hippocampal development and neurodegeneration. *Cell*, 8(3), 206. <https://doi.org/10.3390/cells8030206>
- Hou, Q., Ruan, H., Gilbert, J., Wang, G., Ma, Q., Yao, W. D., & Man, H. Y. (2015). MicroRNA miR124 is required for the expression of homeostatic synaptic plasticity. *Nature Communications*, 6, 10045. <https://doi.org/10.1038/ncomms10045>
- Huang, d., Sherman, B. T., & Lempicki, R. A. (2009a). Bioinformatics enrichment tools: paths toward the comprehensive functional analysis of large gene lists. *Nucleic Acids Research*, 37(1), 1–13. <https://doi.org/10.1093/nar/gkn923>
- Huang, d., Sherman, B. T., & Lempicki, R. A. (2009b). Systematic and integrative analysis of large gene lists using DAVID bioinformatics resources. *Nature Protocols*, 4(1), 44–57. <https://doi.org/10.1038/nprot.2008.211>
- Inohana, M., Eguchi, A., Nakamura, M., Nagahara, R., Onda, N., Nakajima, K., ... Shibutani, M. (2018). Developmental exposure to aluminum chloride irreversibly affects postnatal hippocampal neurogenesis involving multiple functions in mice. *Toxicological Sciences*, 164(1), 264–277. <https://doi.org/10.1093/toxsci/kfy081>
- Jones, P. L., Veenstra, G. J., Wade, P. A., Vermaak, D., Kass, S. U., Landsberger, N., ... Wolffe, A. P. (1998). Methylated DNA and MeCP2 recruit histone deacetylase to repress transcription. *Nature Genetics*, 19(2), 187–191. <https://doi.org/10.1038/561>
- Kaldun, J. C., & Sprecher, S. G. (2019). Initiated by CREB: Resolving gene regulatory programs in learning and memory: Switch in cofactors and transcription regulators between memory consolidation and maintenance network. *BioEssays*, 41(8), e1900045. <https://doi.org/10.1002/bies.201900045>
- Konycheva, G., Dziadek, M. A., Ferguson, L. R., Krägeloh, C. U., Coolen, M. W., Davison, M., & Breier, B. H. (2011). Dietary methyl donor deficiency during pregnancy in rats shapes learning and anxiety in offspring. *Nutrition Research*, 31(10), 790–804. <https://doi.org/10.1016/j.nutres.2011.09.015>
- Kundakovic, M., Gudsruk, K., Franks, B., Madrid, J., Miller, R. L., Perera, F. P., & Champagne, F. A. (2013). Sex-specific epigenetic disruption and behavioral changes following low-dose in utero bisphenol A exposure. *Proceedings of the National Academy of Sciences of the United States of America*, 110(24), 9956–9961. <https://doi.org/10.1073/pnas.1214056110>
- Livak, K. J., & Schmittgen, T. D. (2001). Analysis of relative gene expression data using real-time quantitative PCR and the $2^{-\Delta\Delta C_T}$ method. *Methods*, 25(4), 402–408. <https://doi.org/10.1006/meth.2001.1262>
- Lugert, S., Basak, O., Knuckles, P., Haussler, U., Fabel, K., Götz, M., ... Giachino, C. (2010). Quiescent and active hippocampal neural stem cells with distinct morphologies respond selectively to physiological and pathological stimuli and aging. *Cell Stem Cell*, 6(5), 445–456. <https://doi.org/10.1016/j.stem.2010.03.017>
- Mantamadiotis, T., Lemberger, T., Bleckmann, S. C., Kern, H., Kretz, O., Martin Villalba, A., ... Schütz, G. (2002). Disruption of CREB function in brain leads to neurodegeneration. *Nature Genetics*, 31(1), 47–54. <https://doi.org/10.1038/ng882>
- Masiulis, I., Yun, S., & Eisch, A. J. (2011). The interesting interplay between interneurons and adult hippocampal neurogenesis. *Molecular Neurobiology*, 44(3), 287–302. <https://doi.org/10.1007/s12035-011-8207-z>
- Mateus-Pinheiro, A., Alves, N. D., Patrício, P., Machado-Santos, A. R., Loureiro-Campos, E., Silva, J. M., ... Pinto, L. (2017). AP2γ controls adult hippocampal neurogenesis and modulates cognitive, but not anxiety or depressive-like behavior. *Molecular Psychiatry*, 22(12), 1725–1734. <https://doi.org/10.1038/mp.2016.169>
- Minatohara, K., Akiyoshi, M., & Okuno, H. (2016). Role of immediate-early genes in synaptic plasticity and neuronal ensembles underlying the memory trace. *Frontiers in Molecular Neuroscience*, 8, 78. <https://doi.org/10.3389/fnmol.2015.00078>
- Moutinho, D., Veiga, S., & Requena, J. R. (2020). Human VGF-derived antidepressant neuropeptide TLQP62 promotes SH-SY5Y neurite outgrowth. *Journal of Molecular Neuroscience*, 70(8), 1293–1302. <https://doi.org/10.1007/s12031-020-01541-8>
- Mueller, B. R., & Bale, T. L. (2008). Sex-specific programming of offspring emotionality after stress early in pregnancy. *Journal of Neuroscience*, 28(36), 9055–9065. <https://doi.org/10.1523/JNEUROSCI.1424-08.2008>

- OECD, 2007. Organisation for economic co-operation and development, 2007. OECD Guidelines for the testing of chemicals, Section 4. Test no. 426: Developmental neurotoxicity study, OECD publishing, Paris, France.
- Pak, J. S., DeLoughery, Z. J., Wang, J., Acharya, N., Park, Y., Jaworski, A., & Özkan, E. (2020). NELL2-Robo3 complex structure reveals mechanisms of receptor activation for axon guidance. *Nature Communications*, 11(1), 1489. <https://doi.org/10.1038/s41467-020-15211-1>
- Pawluski, J. L., Brummelte, S., Barha, C. K., Crozier, T. M., & Galea, L. A. (2009). Effects of steroid hormones on neurogenesis in the hippocampus of the adult female rodent during the estrous cycle, pregnancy, lactation and aging. *Frontiers in Neuroendocrinology*, 30(3), 343–357. <https://doi.org/10.1016/j.yfrne.2009.03.007>
- Quach, T. T., Auvergnon, N., Khanna, R., Belin, M. F., Kolattukudy, P. E., Honnorat, J., & Duchemin, A. M. (2018). Opposing morphogenetic defects on dendrites and mossy fibers of dentate granular neurons in CRMP3-deficient mice. *Brain Sciences*, 8(11), 196. <https://doi.org/10.3390/brainsci8110196>
- Rodríguez-Peña, A. (1999). Oligodendrocyte development and thyroid hormone. *Journal of Neurobiology*, 40(4), 497–512. [https://doi.org/10.1002/\(sici\)1097-4695\(19990915\)40:4<497::aid-neu7>3.0.co;2-#](https://doi.org/10.1002/(sici)1097-4695(19990915)40:4<497::aid-neu7>3.0.co;2-#)
- Sakamoto, K., Karelina, K., & Obrietan, K. (2011). CREB: A multifaceted regulator of neuronal plasticity and protection. *Journal of Neurochemistry*, 116(1), 1–9. <https://doi.org/10.1111/j.1471-4159.2010.07080.x>
- Sasidharan Nair, V., Saleh, R., Toor, S. M., Taha, R. Z., Ahmed, A. A., Kurer, M. A., ... Elkord, E. (2020). Transcriptomic profiling disclosed the role of DNA methylation and histone modifications in tumor-infiltrating myeloid-derived suppressor cell subsets in colorectal cancer. *Clinical Epigenetics*, 12(1), 13. <https://doi.org/10.1186/s13148-020-0808-9>
- Shibutani, M. (2015). Hippocampal neurogenesis as a critical target of neurotoxicants contained in foods. *Food Safety*, 3(1), 1–15. <https://doi.org/10.14252/foodsafetyfscj.2014038>
- Shibutani, M., Woo, G. H., Fujimoto, H., Saegusa, Y., Takahashi, M., Inoue, K., ... Nishikawa, A. (2009). Assessment of developmental effects of hypothyroidism in rats from in utero and lactation exposure to anti-thyroid agents. *Reproductive Toxicology*, 28(3), 297–307. <https://doi.org/10.1016/j.reprotox.2009.04.011>
- Shiraki, A., Saito, F., Akane, H., Takeyoshi, M., Imatanaka, N., Itahashi, M., ... Shibutani, M. (2014). Expression alterations of genes on both neuronal and glial development in rats after developmental exposure to 6-propyl-2-thiouracil. *Toxicology Letters*, 228(3), 225–234. <https://doi.org/10.1016/j.toxlet.2014.04.018>
- Shiraki, A., Tanaka, T., Watanabe, Y., Saito, F., Akahori, Y., Imatanaka, N., ... Shibutani, M. (2016). Immunohistochemistry of aberrant neuronal development induced by 6-propyl-2-thiouracil in rats. *Toxicology Letters*, 261, 59–71. <https://doi.org/10.1016/j.toxlet.2016.08.019>
- Sui, L., & Li, B. M. (2010). Effects of perinatal hypothyroidism on regulation of reelin and brain-derived neurotrophic factor gene expression in rat hippocampus: Role of DNA methylation and histone acetylation. *Steroids*, 75(12), 988–997. <https://doi.org/10.1016/j.steroids.2010.06.005>
- Sun, J., Sun, J., Ming, G. L., & Song, H. (2011). Epigenetic regulation of neurogenesis in the adult mammalian brain. *European Journal of Neuroscience*, 33(6), 1087–1093. <https://doi.org/10.1111/j.1460-9568.2011.07607.x>
- Tanaka, T., Nakajima, K., Masubuchi, Y., Ito, Y., Kikuchi, S., Ideta-Ohtsuka, M., ... Shibutani, M. (2019). Aberrant epigenetic gene regulation in hippocampal neurogenesis of mouse offspring following maternal exposure to 3,3'-iminodipropionitrile. *Journal of Toxicological Sciences*, 44(2), 93–105. <https://doi.org/10.2131/jts.44.93>
- Tozuka, Y., Fukuda, S., Namba, T., Seki, T., & Hisatsune, T. (2005). GABAergic excitation promotes neuronal differentiation in adult hippocampal progenitor cells. *Neuron*, 47(6), 803–815. <https://doi.org/10.1016/j.neuron.2005.08.023>
- Vivar, C., Potter, M. C., & van Praag, H. (2013). All about running: Synaptic plasticity, growth factors and adult hippocampal neurogenesis. *Current Topics in Behavioral Neurosciences*, 15, 189–210. https://doi.org/10.1007/7854_2012_220
- Wang, L., Ohishi, T., Shiraki, A., Morita, R., Akane, H., Ikarashi, Y., ... Shibutani, M. (2012). Developmental exposure to manganese chloride induces sustained aberration of neurogenesis in the hippocampal dentate gyrus of mice. *Toxicological Sciences*, 127(2), 508–521. <https://doi.org/10.1093/toxsci/kfs110>
- Wang, L., Shiraki, A., Itahashi, M., Akane, H., Abe, H., Mitsumori, K., & Shibutani, M. (2013). Aberration in epigenetic gene regulation in hippocampal neurogenesis by developmental exposure to manganese chloride in mice. *Toxicological Sciences*, 136(1), 154–165. <https://doi.org/10.1093/toxsci/kft183>
- Wang, R. H., Chen, Y. F., Chen, S., Hao, B., Xue, L., Wang, X. G., ... Zhao, H. (2018). Maternal deprivation enhances contextual fear memory via epigenetically programming second-hit stress-induced reelin expression in adult rats. *The International Journal of Neuropsychopharmacology*, 21(11), 1037–1048. <https://doi.org/10.1093/ijnp/pyy078>
- Watanabe, Y., Abe, H., Nakajima, K., Ideta-Otsuka, M., Igarashi, K., Woo, G. H., ... Shibutani, M. (2018). Aberrant epigenetic gene regulation in GABAergic interneuron subpopulations in the hippocampal dentate gyrus of mouse offspring following developmental exposure to hexachlorophene. *Toxicological Sciences*, 163(1), 13–25. <https://doi.org/10.1093/toxsci/kfx291>
- Watanabe, Y., Murakami, T., Kawashima, M., Hasegawa-Baba, Y., Mizukami, S., Imatanaka, N., ... Shibutani, M. (2017). Maternal exposure to valproic acid primarily targets interneurons followed by late effects on neurogenesis in the hippocampal dentate gyrus in rat offspring. *Neurotoxicity Research*, 31(1), 46–62. <https://doi.org/10.1007/s12640-016-9660-2>
- Weaver, I. C., Cervoni, N., Champagne, F. A., D'Alessio, A. C., Sharma, S., Seckl, J. R., ... Meaney, M. J. (2004). Epigenetic programming by maternal behavior. *Nature Neuroscience*, 7(8), 847–854. <https://doi.org/10.1038/nn1276>
- Weng, X., Zhou, D., Liu, F., Zhang, H., Ye, J., Zhang, Z., ... Liu, Y. (2014). DNA methylation profiling in the thalamus and hippocampus of postnatal malnourished mice, including effects related to long-term potentiation. *BMC Neuroscience*, 15, 31. <https://doi.org/10.1186/1471-2202-15-31>
- Wiegrefe, C., Simon, R., Peschkes, K., Kling, C., Strehle, M., Cheng, J., ... Britsch, S. (2015). Bcl11a (Ctip1) controls migration of cortical projection neurons through regulation of *Sema3c*. *Neuron*, 87(2), 311–325. <https://doi.org/10.1016/j.neuron.2015.06.023>
- Wu, Y., Song, H., Sun, B., Xu, M., & Shi, J. (2015). DNA methylation of the *EphA5* promoter is associated with rat congenital hypothyroidism. *Journal of Molecular Neuroscience*, 57(2), 203–210. <https://doi.org/10.1007/s12031-015-0603-9>
- Wurzman, R., Forcelli, P. A., Griffey, C. J., & Kromer, L. F. (2015). Repetitive grooming and sensorimotor abnormalities in an ephrin-A knockout model for autism spectrum disorders. *Behavioural Brain Research*, 278, 115–128. <https://doi.org/10.1016/j.bbr.2014.09.012>
- Xu, J., He, G., Zhu, J., Zhou, X., St Clair, D., Wang, T., & Zhao, X. (2014). Prenatal nutritional deficiency reprogrammed postnatal gene expression in mammal brains: implications for schizophrenia. *The International Journal of Neuropsychopharmacology*, 18(4), pyu054. <https://doi.org/10.1093/ijnp/pyu054>
- Zhang, Y., Fan, Y., Yu, X., Wang, X., Bao, S., Li, J., ... Teng, W. (2015). Maternal subclinical hypothyroidism impairs neurodevelopment in rat offspring by inhibiting the CREB signaling pathway. *Molecular Neurobiology*, 52(1), 432–441. <https://doi.org/10.1007/s12035-014-8855-x>
- Zhao, C., Deng, W., & Gage, F. H. (2008). Mechanisms and functional implications of adult neurogenesis. *Cell*, 132(4), 645–660. <https://doi.org/10.1016/j.cell.2008.01.033>

Zhu, G., Okada, M., Yoshida, S., Ueno, S., Mori, F., Takahara, T., ... Hirose, S. (2008). Rats harboring S284L *Chrna4* mutation show attenuation of synaptic and extrasynaptic GABAergic transmission and exhibit the nocturnal frontal lobe epilepsy phenotype. *Journal of Neuroscience*, 28(47), 12465–12476. <https://doi.org/10.1523/JNEUROSCI.2961-08.2008>

SUPPORTING INFORMATION

Additional supporting information may be found online in the Supporting Information section at the end of this article.

How to cite this article: Kikuchi S, Takahashi Y, Ojio R, et al. Identification of gene targets of developmental neurotoxicity focusing on DNA hypermethylation involved in irreversible disruption of hippocampal neurogenesis in rats. *J Appl Toxicol*. 2021;41:1021–1037. <https://doi.org/10.1002/jat.4089>